Journal of the Australian Ceramic Society
https://doi.org/10.1007/s41779-024-01020-y

RESEARCH

Structure-property relationship and emerging applications of nano- and micro-sized fillers reinforced sialon composites: a review

Olugbenga Ogunbiyi[1] · Tamba Jamiru[1] · Gbolahan Joseph Adekoya[2] · Azeez Lawan Rominiyi[3]

Received: 24 September 2023 / Revised: 3 March 2024 / Accepted: 7 April 2024
© The Author(s) 2024

Abstract

Oxonitridoaluminosilicates (SiAlON) are renowned in advanced ceramics for their exceptional properties: high temperature stability, excellent oxidation resistance, and good wear resistance. Incorporating micro- and nano-sized fillers into SiAlON matrices enhances their properties, yielding SiAlON composite materials with superior mechanical, tribological, and thermal characteristics. This review examines fabrication techniques for producing SiAlON micro/nanocomposites and the structure-property relationships governing their performance across different phase compositions (β, α, X, and O-phases). A comprehensive literature review scrutinized fabrication techniques and structure-property relationships from various databases and scholarly articles. Although SiAlON composites with micro/nano inclusions hold promise across applications, understanding their fabrication processes, structure-property relationships, and potential applications in different fields is crucial. The review highlights diverse fabrication techniques for SiAlON micro/nanocomposites and provides insights into their structure-property relationships. Additionally, emerging applications in structural domains, cutting tools, coatings, corrosion protection, solar cells, LEDs, biomedical realms, and filtration membranes are discussed. This review is a valuable resource for researchers and engineers interested in designing SiAlON products tailored for sophisticated applications. It emphasizes understanding fabrication processes and structure-property relationships to unlock SiAlON-based materials' full potential across industries.

Keywords SiAlON · Micro/nanofillers · Structure · Emerging applications

Introduction

SiAlON ceramics, a family of cutting-edge materials, have outstanding qualities, including high temperature stability, strong oxidation resistance, and moderate wear resistance. These properties have made them popular for use in various structural and industrial, coupled with engineering applications, such as refractories, cutting tools, heat insulators, and gas turbines. SiAlON ceramics exist in two main types: α-SiAlON ($A_zSi_{12-(x+y)}Al_{x+y}O_yN_{16-y}$, $0 < z \leq 2$)) and β-SiAlON ($Si_{6-z}Al_zO_zN_{8-z}$, $0 < z < 4.2$)), derived from the structural modification of α-Si_3N_4 and β-Si_3N_4, respectively. While α-SiAlON displays a morphology characterized by equiaxed grains, resulting in enhanced hardness and corrosion resistance, it has reduced fracture toughness compared to β-SiAlON, which has elongated grains. Other types include the O'-SiAlON ($Si_{2-z}Al_zO_{1+z}N_{2-z}$, $0 < z < 0.3$)), the X-SiAlON ($Si_{2-z}Al_{1-z}O_zN_{1-z}$, $z = 0.04/0.3$)), the H-SiAlON ($SiAl_3O_2N_3$, $SiAl_5O_2N_5$) and R-SiAlON ($SiAl_4O_2N_4$, $SiAl_6O_2N_6$) [1–5].

While SiAlON ceramics offer appealing properties, their application in specific contexts like cutting tools is constrained by the need for enhanced wear resistance. Moreover, during the sintering phase, glassy phases tend to form at grain boundaries in SiAlON ceramics, thereby limiting their performance at high temperatures. Additionally, although α-SiAlON is harder than β-SiAlON, it displays inferior

✉ Olugbenga Ogunbiyi
olugbengaogunbiyi@gmail.com

[1] Department of Mechanical and Mechatronics Engineering, Tshwane University of Technology, Pretoria 0001, South Africa

[2] Department of Chemical, Metallurgical and Materials Engineering, Faculty of Engineering and the Built Environment, Tshwane University of Technology, Pretoria 0001, South Africa

[3] Department of Mechanical and Industrial Engineering, Faculty of Engineering and the Built Environment, University of Johannesburg, Doornfontein Campus, Johannesburg 2028, South Africa

Published online: 19 April 2024

strength and toughness properties. Researchers have sought to overcome these limitations by adding second-phase particles, such as metallic (e.g., Cu, Sn, Nb, Mo, Fe, and Ni), ceramic (e.g., WC, ZrO_2, AlN, $ZrSi_2$, ZrC, Y_2O_3, ZrN, $TaSi_2$, VC, $MoSi_2$, Si_3N_4, HfN, and SiC), and nanofillers (e.g., graphene and CNT) additives to control grain growth and improve toughness, wear resistance, and electrical conductivity of SiAlON ceramics. This approach enhances the features of SiAlON ceramics, resulting in SiAlON composite materials with superior mechanical, tribological, and thermal properties [3, 6–17]. One of their main advantages is the ability to tailor SiAlON composites for specific applications by exploring various filler materials and adjusting their size and form. For instance, adding graphene improves electrical conductivity, making them suitable for electronics and sensors, while incorporating nitrides like TiN and ZrN enhances wear resistance, making them ideal for cutting tools and wear-resistant applications [6, 7].

SiAlON composites exhibit improved mechanical and electrical properties, making them promising for diverse applications. Their excellent thermal stability and electrical conductivity have sparked interest in utilizing them for solar cells and light-emitting diodes (LEDs) [18–21]. Furthermore, in biomedical fields, SiAlON composites are being studied for drug delivery and tissue engineering due to their biocompatibility and controlled drug release capabilities. Additionally, their stability and corrosion resistance make them attractive for applications in filtration membranes [22–25].

Despite the many potential applications of SiAlON composites with micro/nano inclusions, some challenges still need to be addressed to realize their potential fully. One of the main challenges is the difficulty in fabricating these materials with a uniform distribution of the micro/nano inclusions and controlling the size and shape of these inclusions. In addition, understanding of the processes by which the micro/nano inclusions improve the properties of the SiAlON matrix is lacking, and more research is needed to fully understand the structure-property relationships of these materials [26, 27].

The objective of this study is to provide a comprehensive analysis of the structure-property relationships of SiAlON nanocomposites with different phase compositions. Additionally, the study aims to highlight the emerging applications of SiAlON composites with micro/nano inclusions across various fields, including structural materials, cutting tools, coatings and corrosion protection, solar cells and LEDs, biomedical applications, and filtration membranes. This review seeks to understanding the mechanisms by which the micro/nano inclusions enhance the properties of the SiAlON matrix. Ultimately, the study aims to provide insights into optimizing SiAlON-based materials for diverse high-performance applications [19, 21, 24, 28].

Fabrication techniques for SiAlON-based composites

SiAlON composites consisting of silicon, aluminium, oxygen, nitrogen, and other fillers are notable for their exceptional strength, high temperature resistance, and hardness. They exhibit different phase compositions, including β-phases [29], α-phases [30], X-phases [31], and O-phases [32] (Fig. 1). These features make SiAlON composites desirable for various engineering applications, including wear-resistant coatings, cutting tools, and structural components. SiAlON composites can be manufactured using different fabrication techniques, which can be classed into quite a few types based on their working principle or method of operation. Several techniques to create SiAlON-based composites can be divided into three main categories: powder metallurgy, reactive processing techniques, and other advanced techniques such as combustion synthesis [33, 34].

Powder metallurgy techniques

Powder metallurgy stands out as a prominent method for developing SiAlON composites. This approach involves blending and shaping silicon, aluminum, oxide, or nitride powders, followed by sintering at high temperatures to yield the final composite. Various techniques within powder metallurgy have been devised for SiAlON composite fabrication, encompassing hot pressing, spark plasma sintering, electric current-assisted sintering, gas pressure sintering, microwave sintering, pressureless sintering, and

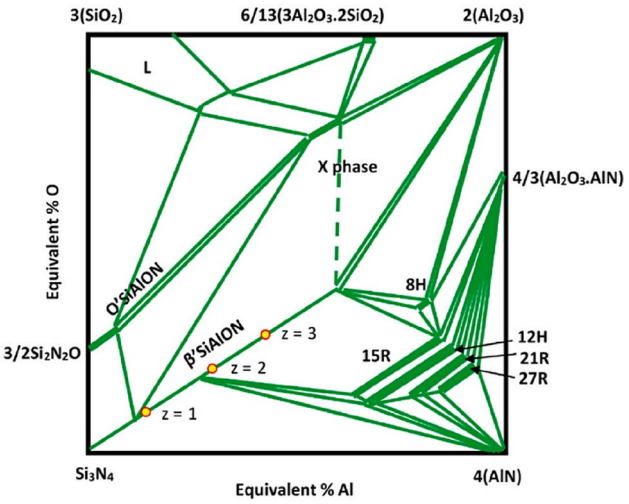

Fig. 1 SiAlON phase behaviour diagram showing the β-, X-, O-phases [35]

liquid phase sintering [10, 36–38]. These methods offer simplicity and versatility in producing a diverse array of shapes and sizes for SiAlON composites (Table 1).

Hot pressing, a powder metallurgy technique, involves compacting powders under high pressure and heating them to promote bonding. This method finds utility in producing materials with high strength and hardness, including SiAlON composites [10, 37, 39]. Notably, Joshi et al. [40] demonstrated the fabrication of transparent Mg-α/β-SiAlON:Ba^{2+} ceramics with notable mechanical properties using hot press sintering [40]. Additionally, Shan et al. [38] successfully developed dense Y^{3+}-doped α-SiAlON/BN composite ceramics via hot pressing, exhibiting enhanced flexural strength at high temperatures [38].

On the other hand, microwave sintering presents an efficient alternative within powder metallurgy, utilizing microwaves to sinter powder beds and achieve particle bonding (Fig. 2a-e). This technique offers reduced sintering times and temperatures compared to conventional methods, along with the potential for unique microstructures [41–44]. Canarslan et al. [1, 8] demonstrated the utility of microwave sintering in creating low-temperature SiAlON/TiN composites, exhibiting improved mechanical properties with 17% TiN. Similarly, microwave sintering has been applied to fabricate SiAlON/TiN composites with enhanced density and mechanical characteristics [8].

Interestingly, spark plasma sintering (SPS) involves the generation of sparks within a powder bed under pressure and electric current, leading to rapid heating and sintering. This method enables the synthesis of SiAlON composites with quicker sintering at lower temperatures compared to other techniques [45, 46]. However, SPS may induce the formation of the X-phase in SiAlON, impacting its microstructure and properties [6, 46–48]. For instance, Nekouee and Khosroshahi [49] successfully produced fully dense β-SiAlON/TiN composites using SPS, exhibiting superior mechanical properties (comprising hardness alongside fracture toughness values of 14.6 GPa and 6.3 MPa $m^{1/2}$, respectively) attributed to crack deflection and even TiN dispersion.

Meanwhile, electric current-assisted sintering (ECAS) employs an electric current to generate heat within a powder bed, facilitating particle bonding. While less commonly used, ECAS can yield SiAlON composites with high strength and hardness. Smirnov et al. [50] utilized ECAS to fabricate β-Si_5AlON_7-TiN ceramic composites with notable relative density [50].

Similarly, gas pressure sintering (GPS) involves heating a compressed powder bed under pressure to promote particle bonding. This method has been utilized to produce SiAlON composites with high strength and hardness [51]. For example, GPS was employed to develop SiAlON-ZrN composites, the study investigated the effects of pressure on sintering and the properties of the composite. Sintering under 1.0 MPa resulted in enhanced density and better mechanical traits compared to 0.4 MPa. By adding ZrN, the hardness of the SiAlON matrix increased up to 30%, reaching a peak of 16.16 GPa at 20% ZrN content. Furthermore, a maximum fracture toughness of 5.41 MPa•$m^{1/2}$ was attained with 50% ZrN, although higher concentrations led to decreased hardness but improved fracture toughness [52].

While pressureless sintering, a technique where a compressed powder bed is heated without external pressure, is effective in producing SiAlON composites with high strength and hardness. This method has been applied to fabricate various SiAlON composites, demonstrating enhanced density and mechanical properties [53]. For example, β-SiAlON composites with additives like $TiC_{0.3}N_{0.7}$ and Al_2O_3-AlN-Y_2O_3 were fabricated using pressureless spark plasma sintering, resulting in high density, fracture toughness, and Vickers hardness [53]. Similarly, β-Sialon (z = 2)/ZrN/ZrON-based composite ceramics were produced by pressureless sintering, showing exceptional oxidation resistance and a microstructure comprising evenly distributed β-Sialon(z = 2), ZrN, and ZrON particles when sintered at 1550°C for 1 hour [54].

Reactive processing techniques

Reactive processing techniques encompass a set of methods aimed at synthesizing materials by inducing reactions between starting materials or precursors to yield desired compounds or compound mixtures. In the realm of SiAlON composite fabrication, these techniques offer diverse approaches, including reaction bonding, aluminothermic processes, carbothermal reduction nitridation, percussion infiltration, and pyrolysis.

Reaction bonding involves the heating of a reactant material on a substrate to foster bonding, resulting in SiAlON composites endowed with excellent mechanical properties. For instance, Yin and Jones [52] employed this method to fabricate SiAlON-ZrN composites, showcasing superior densification and mechanical characteristics under elevated pressures. The study examined the impact of applied pressure on composite characteristics, revealing that composites sintered under 1.0 MPa displayed superior densification and remarkable mechanical properties, with maximum hardness observed at 20% ZrN and highest fracture toughness at 50% ZrN, compared to those sintered under 0.4 MPa [52].

Aluminothermic processes provide a means to synthesize SiAlON composite materials through reactions among starting materials at high temperatures. This approach allows for precise control over composition and microstructure, rendering it suitable for a variety of applications [5, 18, 55, 56]. Kovziridze et al. [5] utilized nitroaluminothermic procedures to manufacture SiAlON composites with superior

Table 1 The summary of the preparation methods for SiAlON composites

Species	Fabrication Technique	Application	Remark	Ref.
β-Si_5AlON_7, h-BN, β-SiC, and TiN	Combustion synthesis/ spark plasma sintering	Strong thermal shock ceramic composites	Fast and energy-efficient techniques. High relative density (> 95%), strong flexural properties (up to 400 MPa)	[77]
ZrN–Sialon	Carbothermal reduction–nitridation	-	The reaction temperature has a significant impact on the final phase composition.	[63]
β-Sialon-ZrN	Reaction bonding and gas pressure sintering process	For machining tools.	Possesses good wear and electrical conductivity	[51, 52]
β-Sialon/ZrN/ZrON	In-situ carbothermal reduction−nitridation, pressureless sintering	Engineering ceramics, refractory materials, and cutting tools	Good corrosion, high strength, and hardness	[54, 78]
β -SiAlON–ZrO_2	Microwave sintering	-	Good densification, phase transformation, microstructure evolution and hardness	[42]
Sialon-ZrN	Two-step sintering/ Combination of reaction bonding and post-gas-pressure sintering	Cutting tools	Good wear and hardness.	[4, 79]
SiC–Sialon–ZrN	Carbothermal reduction nitridation (CRN)	Iron-making	In samples produced by adding ZrN, the penetrating ability of the slag resistance increased.	[80]
TiN reinforced Sialon	LABOX-3010KF furnace in a vacuum atmosphere (Mixing)	For high-temperature applications	Good mechanical properties and tribological behaviours	[81]
ZrB_2-SiC-SiAlON	Hot pressing	-	-	[10]
β-SiAlON–ZrO_2	Nitriding electric furnace.	Biomaterials material for wound-healing.	It has good physicochemical and biological properties	[82]
β-SiAlON–SiC	Liquid phase sintering	-	-	[83]
αı/βı-SiAlON-TiN	Planetary milling	Tribological properties	-	[84]
SiAlON-doped ZrB_2–SiC	Hot pressing and pressureless sintering/Liquid phase sintering	-	Sintered at 1900 °C.	[37]
Ca-α SiAlON	Spark plasma sintering (SPS)/Carbothermal reduction nitridation process	Cutting tools	The optimal amount of carbon in the precursor, 2 wt% Ca-α-SiAlON seed, increases purity and morphology.	[85, 86]
GNPs -SiAlON	Spark plasma sintered	-	It has good hardness, modulus of elasticity, fracture toughness, wear rate and electrical conductivity.	[15]
TiO_2–SiAlON	Atmospheric plasma spraying (APS)	Wear resistant materials	Good hardness, modulus of elasticity, fracture toughness, and wear rate	[87]
B-SiAlON-cBN	Spark plasma sintering	Cutting tool materials	Good density and Vickers hardness.	[46, 88]
cBN-SiAlON	Spark plasma sintering	-	-	[89]
Epoxy-SiAlON	Electrostatic Spraying	Coating for petrochemical and oil/gas pipelines	It has good corrosion resistance.	[90]
Sialon–Si_3N_4	Hot-pressing	Cutting tools and wears	-	[91]

Table 1 (continued)

Species	Fabrication Technique	Application	Remark	Ref.
BN-SiO_2 -SiAlON	Hot-pressing	For plasma erosion resistance application	Plasma erosion rate decreases then increases with AlN addition; erosion pits are observed on the surface after sputtering.	[92]
Al_2O_3–SiO_2–â-SiAlON–TiC–Dy_2O_3	Spark-plasma sintering	-	SPS @60 MPa in the range of 1200 – 1600 °C	[93]
27R-SiAlON polytype/AlN	Spark plasma sintering	-	Good density, Vickers hardness, indentation and fracture toughness	[94]
Si_3N_4/CaO-doped SiAlON, Si_3N_4/Yb_2O_3-doped SiAlON	Ultrasonic probe sonication and Spark plasma sintering	Long-lasting cutting tools	-	[95]
β-SiAlON–BN	SPS, infiltration-mediated combustion synthesis (CS)	Pouring metal melts and liming plates. Machinable ceramics	Good thermal shock and corrosion resistance.	[96, 97]
α-SiAlON/BN	Hot Pressing	Machining	Flexural strength	[38]
cBN/SiAlON	spark plasma sintering	-	-	[98]
β-Sialon-cBN	High temperature (1700 °C) and high pressure (5 GPa) sintering	Machining	-	[99]
cBN/β-SiAlON	Spark plasma sintering	Machining	-	[47]
TiN-Sialon-Corundum	Aluminothermic reduction nitridation (ARN) method	-	-	[100]
Bauxite-based β-SiAlON	-	-	Oxidation kinetics	[101]
β-SiAlON/Y-Si-Al-O-N	-	Wettability of interlayer	-	[102]
WC/d α-Sialon	SPS technique /Liquid phase sintering	Structural applications	-	[102–104]
SiC/SiAlON	Magnetron sputtering	Industrial application		[105]
Mg-doped sialon	Hot pressed (1850 °C for 1 h, employing La_2O_3 as a sintering additive)	-	Good mechanical and optical properties	[106]
Ca-α-SiAlON:Eu2+	Gas-pressure sintering	LED applications	-	[20]
Ca-α-SiAlON	Spark plasma sintering		-	[3]
β-SiAlON bonded WC	Spark plasma sintering	Advanced uses for wear parts	-	[107]
15R-SiAlON in Fe_xSi_y-Si_3N_4-Al_2O_3	Ferrosilicon nitride-alumina composites are sinterable at 1800 °C with flowing nitrogen.	-	-	[108]
β-SiAlON/graphene oxide	Dip coating/sintering	For improved separation of the water/oil emulsion and anti-fouling	-	[28]
SiAlON–Al_2O_3	Reaction-bonded sintering	Clinical applications	Excellent biocompatibility.	[24]
β-Sialon-bonded Al_2O_3–C refractories	Sintering and DFT (CASTEP/PBE/GGA)	Thermal shock resistance applications. Membrane distillation, electro-discharge machining (EDM), and composition reinforced phases	The sintered composites possess good heat resistance and thermal shock resistance.	[109–112]
β-Sialon/nanofiber	Nitridation	-	-	[113]
SiAlON–Si_3N_4	Reaction-bonded sintering / direct nitridation	Potential bone repairing material	Good bioactivity	[23]

Table 1 (continued)

Species	Fabrication Technique	Application	Remark	Ref.
Ca-α-Sialon/SiC	Spark plasma-sintering furnace (SPS).	-	-	[114]

physical and mechanical properties, well-suited for high-refractory applications [5].

Carbothermal reduction nitridation (CRN) entails heating a material to high temperatures in a reducing environment to produce nitride compounds [57–64]. This method facilitates the synthesis of SiAlON composites with notable strength and hardness, contingent upon appropriate selection of starting materials and optimization of reaction conditions (Fig. 2g) [2, 33, 60, 65, 66]. Wu et al. [65] demonstrated the fabrication of α-SiAlON powder via CRN, illustrating the influence of starting powder ratios on phase composition and microstructure.

Precursor infiltration and pyrolysis (PIP) involves infiltrating a precursor material into a porous substrate, followed by heating to decompose the precursor and form desired compounds or mixtures [67, 68]. This technique has been leveraged to produce SiAlON composites with enhanced strength and hardness [69, 70]. Li et al. [71] successfully fabricated β-SiAlON/hexagonal boron nitride nanocomposites via PIP (Fig. 2h), revealing improved thermal shock resistance and machinability [72].

Combustion synthesis

Combustion synthesis enables the production of ceramic and composite materials by igniting starting materials to induce chemical reactions. This method offers a means to develop SiAlON-based composites with high strength and hardness [73–76]. Grigoryev et al. [72] utilized combustion synthesis to fabricate β-SiAlON-based composites, demonstrating their potential for applications requiring high resistance to thermal shock and corrosive media.

SiAlON-based composites

β-phases SiAlON based composites with Micro and Nano inclusions

The influence of fillers such as Si_3N_4, SiC, Al_2O_3, TiN, Zirconium-based fillers, cBN, and hBN on α-SiAlON, β-SiAlON, and O-SiAlON composites reveals similarities in their effects across the different structures (Table 2). These fillers generally enhance mechanical properties, including strength, hardness, wear resistance, and thermal stability, regardless of the SiAlON phase. For example, Si_3N_4 contributes to the formation of SiAlON phases and improves mechanical strength [115, 116], while SiC reinforces the composites and enhances hardness and wear resistance [117, 118]. Al_2O_3 improves mechanical properties and wear resistance in all composites [111, 119], while TiN improves hardness and wear resistance. [120, 121] Both cBN and hBN enhance lubricity, reduce friction, and

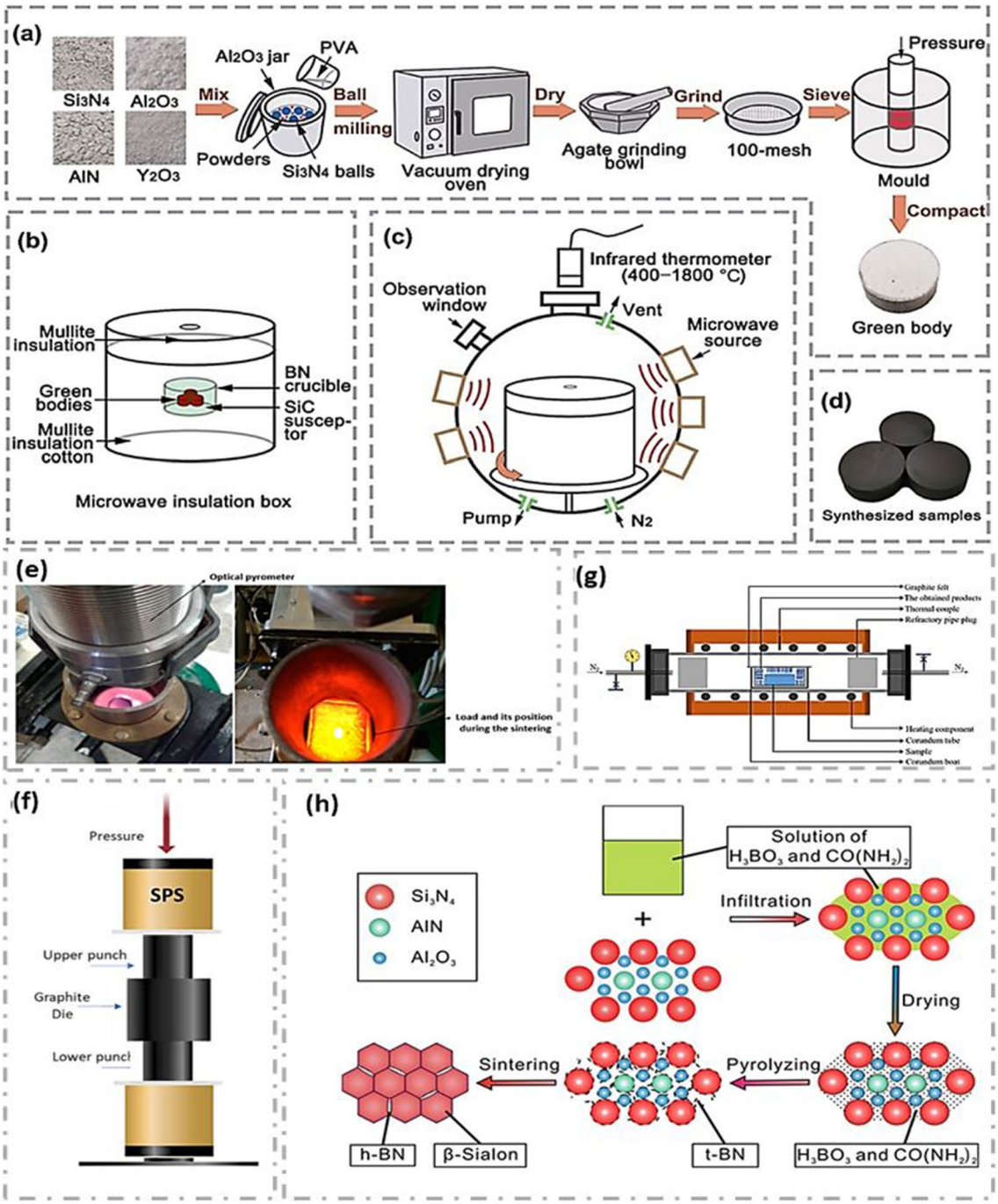

Fig. 2 Illustrations of the green body preparation process, the microwave insulating box, the microwave synthesis system, and the microwave-produced α/β-SiAlON cutting inserts are shown in (**a**), (**b**), (**c**), and (**d**), respectively. Copyright 2022 Springer [41] (**e**) The load's location in the furnace from above during microwave processing. Copyright 2019 MDPI [8] (**f**) SPS process (**g**) The experimental setup for creating β-SiAlON nanostructures and ceramic composite powders made of nitride is shown in a schematic image. Copyright 2019 IOP Publishing Ltd [64] (h) β-SiAlON/h-BN nanocomposite production using the PIP technique Copyright 2015 Elsevier [71]

act as solid lubricants [38, 122, 123]. However, specific variations may exist depending on the composite's phase and composition. The choice between nano- and micro-sized fillers depends on specific application requirements and processing considerations, with nano-sized fillers typically offering superior performance in mechanical and thermal properties, while micro-sized fillers provide better control over microstructural features and processing parameters [118, 124, 125]. In general, integrating these fillers enables customization of SiAlON composites'

Table 2 Comparison of the influence of various fillers on different SiAlON structures

SiAlON Structure	Filler	Influence	Example/Reference
β	Magnesium (Mg)	Enhances high-temperature stability and oxidation resistance	Joshi et al. [40]- Light transmission of about 78% in the IR region (2500 nm) and hardness of 21.4 GPa
β	Titanium (Ti)	Improves mechanical strength and wear resistance	Yurdakul and Turan [120]- Ti-doped SiAlON-based materials for different engineering applications
β	Calcium (Ca)	Enhances thermal conductivity and fracture toughness	
β	Iron (Fe)	Influences magnetic properties and mechanical behavior	Sun et al. [126]- Improved sinterability, flexural strength, and hardness of β-SiAlON composites with Fe_3Al reinforcement
β	Silicon Nitride (Si_3N_4)	Enhances mechanical strength, hardness, and thermal stability	Zheng et al. [115]- Improved toughness and oxidation resistance of β-SiAlON with Si_3N_4 addition
β	Zirconium-based fillers	Enhance sinterability and mechanical properties	Ma et al. [54]- Improved improves the sintering properties and oxidation resistance of SiAlON-ZrN/ZrON composite.
β	Cubic Boron Nitride (cBN)	Enhances hardness and wear performance	Ahmed et al. [122]- Improved mechanical strength with Vickers hardness (HV10) up to 24.0 GPa
β	Hexagonal Boron Nitride (hBN)	It improves lubricity and reduces friction	Shan et al. [38]- Enhanced lubricating properties and flexural strength with hBN inclusion.
β	Titanium-based fillers	Improves various mechanical properties	Yurdakul and Turan [120]- Enhanced wear resistance and mechanical strength with TiN inclusion
β	Al_2O_3-C Refractories	Enhances thermal and mechanical properties	Yin et al. [111]- Improved thermal conductivity and mechanical strength with Al_2O_3-C refractories inclusion
α	Cubic Boron Nitride (cBN)	Enhances hardness and wear performance	Gareth et al. [123]- Increased hardness up to 21 GPa and fracture toughness over 8 MPa m0.5 with cBN inclusion
α	Hexagonal Boron Nitride (hBN)	Enhances lubricity and reduces friction	Shan et al. [38]- Increased flexural strength with hBN inclusion
α	Silicon Nitride (Si_3N_4)	Improves mechanical strength, hardness, and thermal stability	Choi et al. [127]- Increased fracture toughness and density with Y_2O_3 inclusion
α	Silicon Carbide (SiC)	Enhances hardness, wear resistance, and thermal conductivity	Kushan Akin et al. [117]- Improved hardness and fracture toughness with SiC inclusion
α	Alumina (Al_2O_3)	Enhances mechanical properties and wear resistance	Shao et al. [119] - Improved hardness and wear resistance with Al_2O_3 addition
α	Yttrium Oxide (Y_2O_3)	Modifies microstructure and aids sintering	Choi et al. [127]- Improved sinterability and fracture toughness with Y_2O_3 addition
α	Titanium Nitride (TiN)	Improves hardness and wear resistance	Jiang et al. [121] - Enhanced oxidation resistance with TiN inclusion
α	Titanium Dioxide (TiO_2)	Affects optical properties and stability	Yang et al. [128]- Influence on oxidation behavior and phase compositions of O-SiAlON composites with TiN inclusion
O	Silicon Carbide (SiC)	Improves mechanical properties and wear resistance	Kaya et al. [118]- Improved densification and tribomechanical properties with SiC inclusion
O	Titanium Nitride (TiN)	Affects oxidation behavior and phase compositions	Jiang et al. [121] - Enhanced oxidation resistance with TiN inclusion
O	Aluminum Nitride (AlN)	Improves densification, microstructure, and tribomechanical properties	Biswas et al. [94]- Improved wear resistance with AlN inclusion

properties to suit diverse industrial applications, as elaborated in subsequent sections.

β-SiAlON composites with Si_3N_4 fillers

The structural and behavioral attributes of SiAlON composite ceramics hinge primarily upon the relative proportions of constituent elements and the employed processing methodologies [64]. Ceramic inclusions significantly alter the microstructural features and properties of resulting composites. The microstructure of β-SiAlON significantly governs its properties, with Si3N4 fillers exerting a pivotal role in shaping it. Introduction of β-Si3N4 into the precursor mix intricately alters the resultant β-SiAlON's morphology (Fig. 3a-f). For instance, augmenting the molar percentage of β-Si3N4 can transition the structure from fiber-like to rod-like, thereby influencing properties like grain growth, surface area, and oxidation resistance [22, 23].

The optimal molar ratio of β-Si3N4 plays a critical role. At approximately 29.9 mol%, enhanced grain growth and reduced surface area contribute to superior resistance to oxidation. However, excessive Si3N4 content may introduce trade-offs such as diminished mechanical properties or thermodynamic instability in oxidizing environments. Thus, meticulous control over Si3N4 fillers allows tailoring of properties for specific applications, rendering β-SiAlON composites invaluable in high-temperature settings. The incorporation of Si_3N_4 into SiAlON composites yields

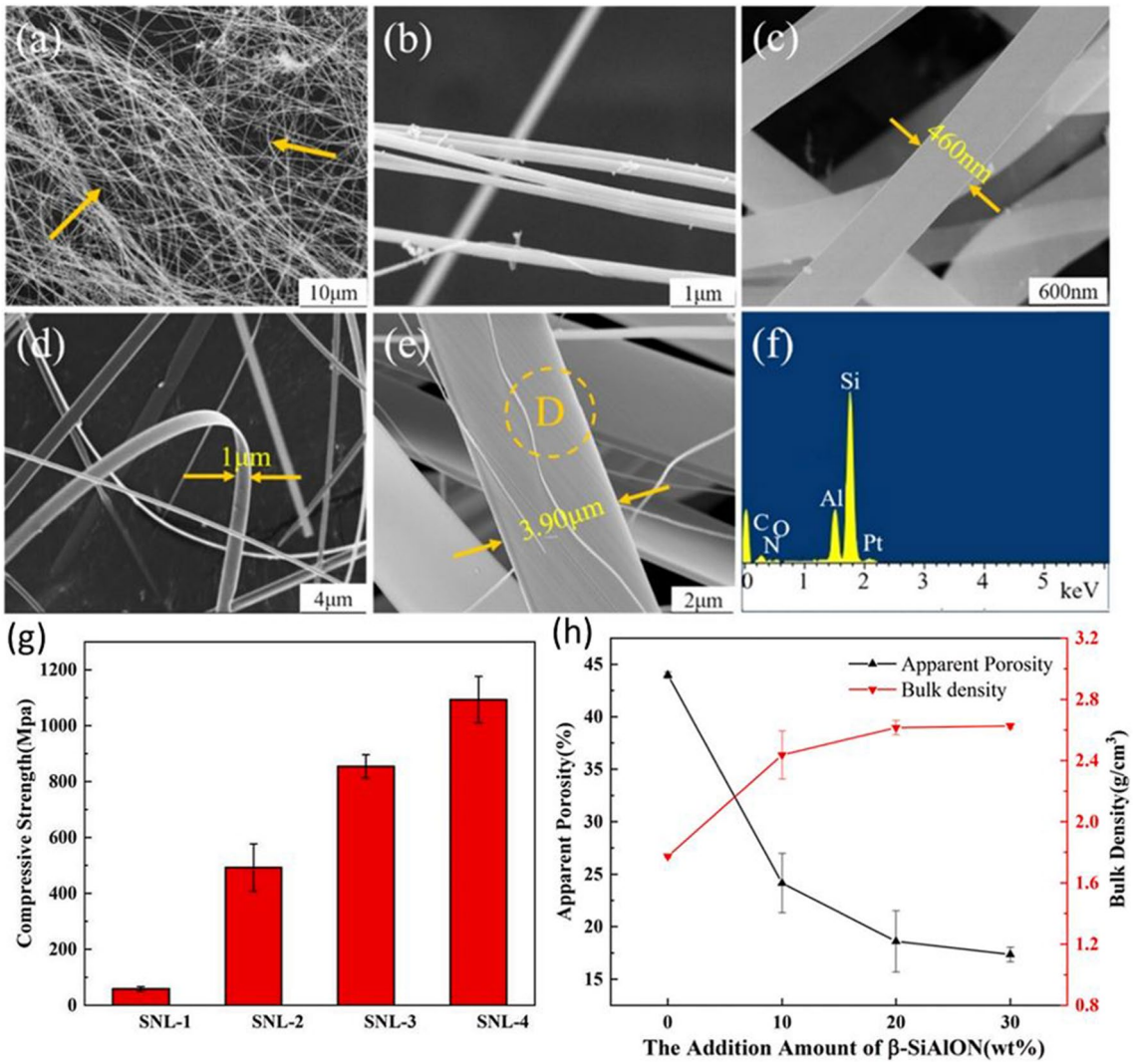

Fig. 3 (**a**-**e**) Micrographs produced using field emission scanning electron microscopy of different Si_3N_4/SiAlON composite nanowires prepared with varying amounts of Al. (**f**) Record of the nanobelts' energy dispersive spectroscopic patterns from location D in Fig. 4e indicated. Copyright 2019 IOP Publishing Ltd [64] Si_3N_4 in SiAlON composite (**g**) Compressive strength properties, and (**h**) The bulk density combined with apparent porosity of the composite made of SiAlON and Si_3N_4 and sintered at 1600°C. Copyright 2022, Elsevier [22]

enhancements in compressive strength, density, and reduced porosity (Fig. 3g & h). Additionally, it markedly improves mechanical, solar absorptance, and thermal properties [22, 129].

In a research by Li et al. [22], Si_3N_4 was incorporated into SiAlON and the primary crystal phase was revealed to be β-Si_3N_4. It was described that the addition of Si_3N_4 caused phase transformation from α-SiAlON to β-SiAlON. The presence of Si_3N_4 boosted the densification of the composite, the bulk density of the material and compressive strength increased while its porosity decreased. The authors observed optimum properties for the developed SiAlON-Si_3N_4 ceramic composite at 30 wt% β-SiAlON content. Furthermore, the embedding of Si_3N_4 into SiAlON also leads to the discharge of ammonia nitrogen in deionized water, which has a bacteriostatic effect that inhibits the proliferation of bacteria.

Bake et al. [35] investigated the influence of nano-and micron-sized Si3N4 particles on the phase characteristics and properties of SPSed β-SiAlON-based composites fabricated at temperatures between 1400 °C and 1700 °C. They realized that the use of amorphous, nanosized Si_3N_4 as a precursor in the synthesis process accelerates the reaction kinetics, resulting in higher values of Vickers hardness and fracture toughness. A similar report was presented by Lv et al. [64] while studying the growth mechanism in 1D β-SiAlON nanostructures alongside β-SiAlON-Si_3N_4 composites fabricated by the reduction nitridation process. However, when micro-sized Si_3N_4 was used as a precursor, the resulting materials displayed slightly lower hardness and fracture toughness values. Nevertheless, they are still comparable to fully dense β′-SiAlONs, which have been sintered using different techniques at substantially greater temperatures for a longer time [35]. Consequently, samples made from nanoscale, amorphous Si_3N_4 exhibited hardness values between 13.4 and 13.8 GPa and a fracture toughness range of 3.5 to 4.6 MPa $m^{1/2}$. In comparison, composites made from microscale β-Si_3N_4 displayed hardness values between 13.9 and 14.4 GPa and a fracture toughness range of 4.3 to 4.5 MPa $m^{1/2}$.

Furthermore, the study carried out by Wu et al. [129] on in-situ β-Sialon/Si_3N_4 ceramic composite prepared at 1580 °C by means of pressureless sintering using Y_2O_3, calcined bauxite, AlN, α- Si_3N_4, and La_2O_3 as sintering additives, showed that the developed composite possesses good mechanical properties, high thermal conductivity, and solar absorptance, alongside excellent thermal shock resistance and oxidation resistance. The composite also exhibits excellent solar heat absorption properties, making it a prospective candidate for use as a solar heat-absorbing material. From the reviewed works, it was generally established that the presence of Si_3N_4 in SiAlON-based composite considerably enhanced the mechanical and thermal properties of the materials, presenting them as attractive for a widespread variety of potential applications.

β-SiAlON composites with Zirconium-based fillers

Zirconium-based fillers, such as ZrN, play a pivotal role in shaping the composition of β-SiAlON composites. Zirconium augments the stability of the composite and significantly contributes to its high-temperature performance. The formation of a solid solution by incorporating zirconium into the crystal lattice of β-Si3N4 results in enhanced mechanical strength and chemical stability.

The microstructure of β-SiAlON undergoes significant alterations owing to the presence of zirconium-based fillers. During sintering, zirconia (ZrO2) reacts with silicon nitride (Si3N4) and aluminum nitride (AlN), giving rise to zirconium nitride (ZrN). These ZrN particles contribute to the composite's microstructure, influencing properties such as grain size, porosity, and phase distribution. Precise control over heating temperature and zirconium content, along with the addition of carbon black, enables tailored microstructure development in the synthesized composites.

The optimal quantity of zirconium-based fillers is crucial. Incremental zirconium content enhances nuclear properties, diminishes the coefficient of thermal expansion, and improves mechanical characteristics. However, excessive zirconium incorporation may lead to trade-offs such as reduced mechanical strength or thermodynamic instability [52]. For instance, Yin and Jones [4] studied the properties of SiAlON-ZrN composites developed by a two-step sintering method. The authors discovered that composites sintered under higher pressure displayed better densification and enhanced mechanical properties, with composite reinforced with 20% ZrN exhibiting the maximum hardness of 16.16 GPa. However, a decrease in hardness was observed at ZrN content higher than 20% due to the weak interfacial bond between the SiAlON matrix and ZrN particles. In these cases, the fracture toughness of the composite may increase, reaching a maximum of 5.41 MPa·$m^{1/2}$ with 40% ZrN. However, the electrical properties of the sintered composites remain unaffected regardless of the adopted sintering techniques. The observed properties of the developed composites were ascribed to the smaller grain size combine with homogeneous microstructure inherited from the processing method since the higher sintering temperatures in the second step can lead to higher relative density, more negligible open porosity, and significantly increased hardness and fracture toughness of the composite.

Yin and Jones [4] and Ma et al. [54] established that the sintering temperature employed affects the structure, composition and properties of the fabricated composite. Ma et al. [54] claim was based on the outcome of their work on SiAlON-ZrN/ZrON composite ceramics using a pressureless

sintering technique at temperatures between 1450 °C and 1550 °C. Their study disclosed that increasing the sintering temperature improves the sintering properties and oxidation resistance of the composite. Dense SiAlON-ZrN/ZrON was achieved at a sintering temperature of 1550 °C for 1 hour. This sample displayed excellent oxidation resistance at 900 °C for 6 hours. The microstructure of the developed composites (Fig. 4a-f) typically consists of ZrN, β-Sialon, and ZrON, with evenly dispersed ZrN combined with ZrON particles on the β-Sialon matrix.

Zhang et al. [82] also observed that introducing ZrO_2 into the β-SiAlON matrix improves the physicochemical and biological properties of the resulting composite ceramics. In addition, they reported that incorporating a small amount of ZrO_2 into the β-SiAlON matrix promotes good adhesion and growth of osteoblast cells on the ceramic surface. Besides, it improves the density, elastic modulus, and flexural strength (Fig. 4g and h). However, it was observed that increasing ZrO_2 contents reduces the porosity of β-SiAlON (Fig. 4g), and excessive amounts of ZrO_2 can have an adverse effect on the cells' wound-healing ability. Hmelov [130] synthesized and studied the properties of SPSed mullite-SiAlON-ZrB_2 materials. The authors observed that increasing the SiAlON concentration impaired sinterability and worsened the sintered materials' physicochemical characteristics at temperatures between 1200 °C and 1600 °C.

Therefore, judicious integration of zirconium-based fillers in β-SiAlON composites facilitates customization of properties for specific applications, rendering them indispensable in high-temperature environments.

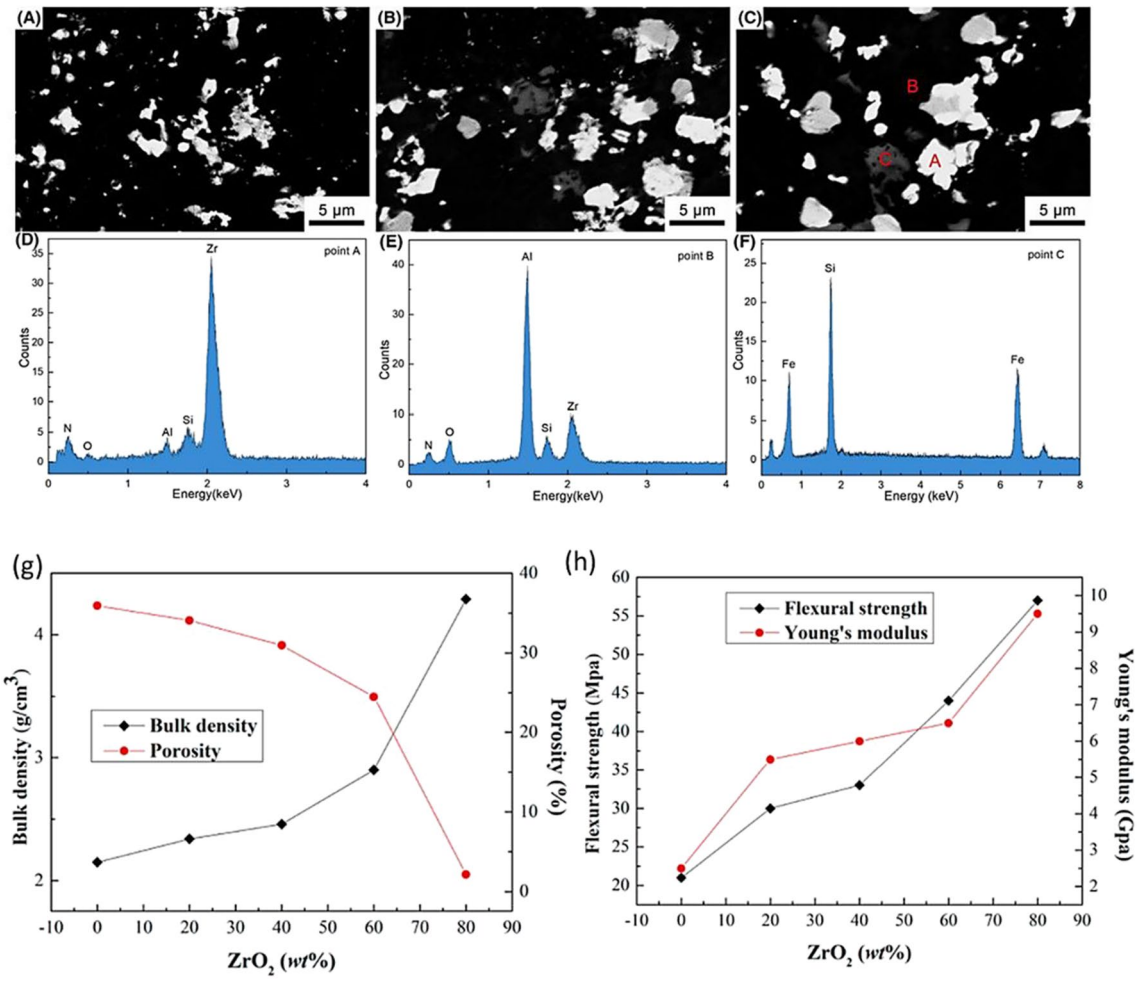

Fig. 4 Backscattered SEM micrographs of SZZCCS samples processed for 1 h at various temperatures (**a**) 1450 °C, (**b**) 1500 °C, (**c**) 1550 °C. The respective EDS analyses at (**d**) 1450 °C, (**e**) 1500 °C, and (**f**) 1550 °C. Copyright 2019 The American Ceramic Society [54], (**g**) the bulk density and porosity, and (**h**) Young's modulus and flexural strength of the β-SiAlON–ZrO_2 composite ceramics. Copyright 2021 Elsevier [82]

β-Sialon composites with boron nitride fillers

Boron nitride (BN) has proven to enhance the structure and properties of β-SiAlON composite materials when used as a filler. Cubic boron nitride (c-BN) alongside hexagonal boron nitride (h-BN) are both commonly used in the production of β-SiAlON composites and have been shown to have varying influences on the structure alongside the composite material's properties [46, 88, 92, 96, 97, 131–135]. The microstructure of β-SiAlON undergoes significant transformations owing to the presence of BN fillers. Fine BN powder leads to improved densification and mechanical properties compared to larger BN particles. The interaction between BN and SiAlON influences grain size, porosity, and phase distribution. Additionally, thermal properties such as thermal conductivity are enhanced in both BN powder-added β-SiAlON composites compared to pristine β-SiAlON. Also, the ability to increase the friction alongside wear resistance of the composite material is one of the main advantages of BN incorporation in β-SiAlON. Yin et al. [131] exhibited that the inclusion of h-BN to SiAlON results in a composite material with a lower friction coefficient and improved lubrication properties. This translates to better friction and wear resistance compared to monolithic SiAlON.

The integration of BN into the composite material has also been revealed to improve the machinability alongside the resistance of β-SiAlON to thermal shock. h-BN, in particular, has a significant impact on these properties. According to Tian et al. [92], the addition of h-BN to SiAlON results in in-situ formed BN-SiO_2, which immensely contributes to the improved resistance of β-SiAlON composite materials to plasma erosion. The authors further reported that when c-BN is used as a filler in SiAlON, it impacts the improved erosion resistance of β-SiAlON/c-BN ceramic composites.

The incorporation of BN in β-SiAlON composite materials (Fig. 5a) has also been shown to impact the composite's densification and mechanical characteristics. Ye et al. [47] prepared cBN/β-SiAlON composites by the SPS process at 1550 °C, 50 MPa for 5 min. It was found that the sintered composites exhibited improved density (Fig. 5b), Vickers hardness, fracture toughness, coupled with the flexural strength compared to pure β-SiAlON. This was attributable to the high density, lack of transformation from cBN to h-BN, and strong interfacial bonds between the cBN grains and the β-SiAlON matrix. Conversely, Wu et al. [99] established that the addition of cBN to β- SiAlON impaired the densification alongside mechanical characteristics of the developed composite materials as the aluminum and oxygen content increased. This effect was observed to be more pronounced with higher z values, which represent the amount of Al atoms that Si atoms in the β-Sialon chemical composition have replaced. Barick and Saha [136] also examined the effects of h-BN incorporation alongside its varied particle sizes on the properties of β-SiAlON ceramic fabricated via the pressureless sintering method at 1800 °C for 4

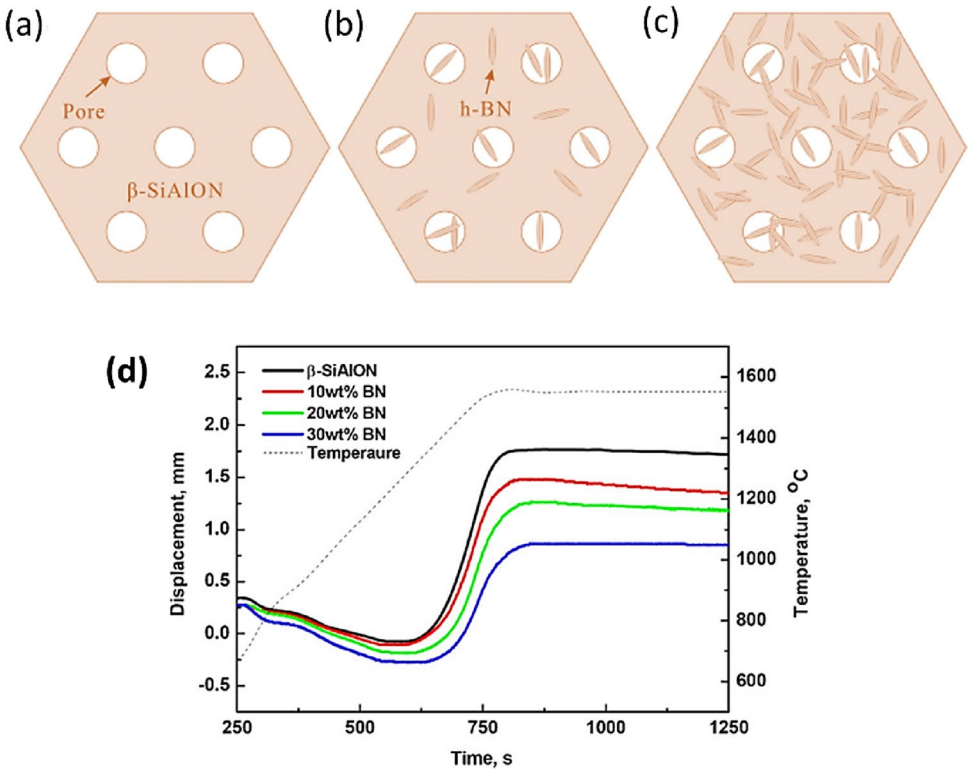

Fig. 5 Graph showing the distribution of h-BN in the SiAlON composites: (**a**) without h-BN, (**b**) with less h-BN, and (**c**) with more h-BN. Copyright 2017 Elsevier [27], (**d**) c-BN/β-SiAlON composite densification curves during the SPS process. Copyright 2010 Elsevier [47]

hours. It was established that the incorporation of h-BN into β-SiAlON ceramic significantly influences the mechanical, microstructure, density, dielectric, and thermal properties of the composite material. The bulk density of β-SiAlON obtained drop from 3.22 g/cm^3 for pure β-SiAlON to 3.05 g/cm^3 and 2.90 g/cm^3 for small and large particle sizes, respectively, when the BN content of the initial composition was increased by up to 5 wt%. Pure β-SiAlON was also shown to have greater Young's modulus, fracture toughness, Vickers hardness, and flexural strength compared to any of the developed composite ceramic materials. Furthermore, improved thermal properties with relatively low dielectric constant were observed in the fabricated β-SiAlON/h-BN composite ceramics than the pure β-SiAlON. Li et al. [27] also reported that adding BN into the β-SiAlON/BN composite improved the flexural strength of the composite material, and consequently obtaining highest flexural strength with 20 wt% BN dosage.

The use of the precursor infiltration and pyrolysis (PIP) process in combination with pressureless sintering was also found to greatly increase the resistance of the composites made of β-SiAlON and h-BN to thermal shock while only slightly decreasing the strength and hardness of the materials. This makes the composite a promising material for high-temperature environments [71, 72]. According to Li et al. [71], adding h-BN to β-SiAlON via a PIP route and pressureless sintered at 1750 °C was found to enhance the machinability and thermal shock resistance of the composite material. In this case, the h-BN particles were observed to be nanoflake-like in shape and distributed homogeneously throughout the β-SiAlON matrix. In a similar work by the authors [72], high strength, remarkable thermal shock resistance and density comparable to that of the pressureless sintered β-SiAlON were obtained in β-SiAlON/h-BN prepared through PIP combined with pressureless sintering.

Overall, the introduction of BN to β-SiAlON composite materials has been shown to have several beneficial effects on the composition and characteristics, including improved friction and wear resistance, machinability, thermal shock resistance, plasma erosion resistance, and mechanical attributes of the developed composite materials. The specific impacts of BN on the structure and properties of SiAlON composite materials will depend on the type, characteristics and concentration of BN utilized, as well as the processing conditions and methods employed to produce the composite material.

β-SiAlON composites with Titanium-based fillers

Titanium-based fillers, such as TiCN, TiO_2, and TiN, have significantly improved the properties of SiAlON composites when added in small amounts [53, 137–140]. Moreover, the microstructure of β-SiAlON is notably influenced by the presence of TiN fillers. TiN particles interact with SiAlON, impacting grain size, porosity, and phase distribution. Proper control of sintering parameters allows for tailored microstructures. Typically, TiN inclusions are found at grain boundaries but may not form a continuous network within the SiAlON matrix. For instance, β-SiAlON/$TiC_{0.3}N_{0.7}$ composite ceramic comprising 2.0–7.5 wt.% $TiC_{0.3}N_{0.7}$ and Al_2O_3–AlN–Y_2O_3 additives were prepared using pressureless SPS at 1550 °C by Li et al. [53]. The authors observed that the produced composites exhibited homogeneously dispersed $TiC_{0.3}N_{0.7}$ particles within the closely packed β-SiAlON grains, which culminated in the attainment of high relative density, Vickers hardness alongside fracture toughness of 98%, 14.53 GPa and 7.20 MPa m$^{1/2}$, respectively, in composite reinforced with 5 wt% $TiC_{0.3}N_{0.7}$. Fully densified β-SiAlON/5 wt% $TiC_{0.3}N_{0.7}$ composite with improved Vickers hardness (15.87 GPa) alongside fracture toughness (7.44 MPa m$^{1/2}$) was reported by further SPS at 1400 °C and 24 MPa. The observed properties improvement of the pressureless SPS compared to the pressurized SPS was ascribed to the absence of non-uniform, uniaxial pressure exerted by the punches during the normal pressurized SPS. Yurdakul et al. [141] examined the electrical properties of α-β SiAlON granules coated with TiCN powder (Fig. 6a & c). Subsequently, they were sintered using the gas pressure sintering (GPS) technique at 1990 °C and 10 MPa nitrogen gas pressure. This process resulted in the creation of a continuous 3D network that conducts electricity. It was reported that the TiCN grains did not retain their original composition after sintering. Also, the migration of Ti from TiCN grains into the α-β-SiAlON and triple junction phases was revealed by the analysis of the Ti:C:N ratios and TEM imaging of the α-β SiAlON/TiCN composite. It was established that the high electrical conductivity of the α-β SiAlON/TiCN composite was due to the presence of Ti in the SiAlON crystal lattice. Canarslan et al. [1] examined the dielectric properties of the initial powders and the characteristics of the microwave sintered α-β SiAlON composite reinforced with 17 wt%TiN at 1300 °C for 30 mins. The authors found that incorporating TiN into α-β SiAlON composites resulted in higher peak sintering temperatures and caused increased microwave absorption characteristics. This led to a decrease in the α:β ratio and an improvement in the mechanical properties, particularly the fracture toughness of the composites (Fig. 6c). Acikbas et al. [142] studied the microstructure, densification, mechanical properties and thermal shock resistance of α:β-SiAlON reinforced with 10, 17, and 25 wt%TiN and sintered by a two-step gas pressure sintering cycle. Enhanced microstructure and fracture toughness were observed in the developed composites due to the presence of TiN in the matrix. Maximum fracture toughness was achieved for composite reinforced with 25wt% TiN. An investigation of the tribological properties of the developed

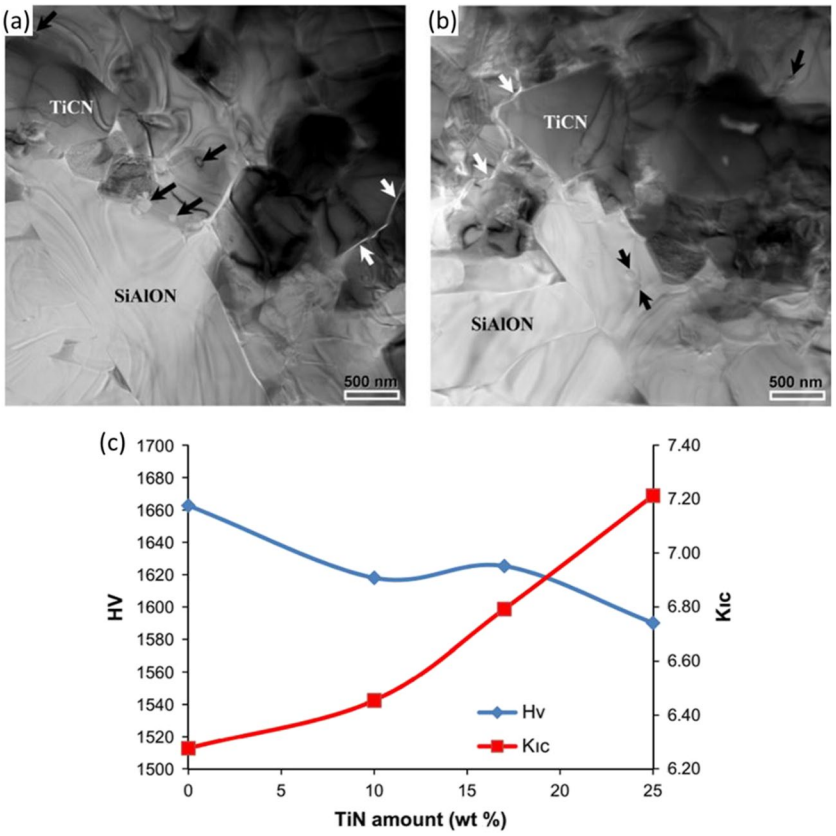

Fig. 6 (**a** and **b**) Bright-field (BF) TEM nanographs captured from various angles of the SiAlON/TiCN composite [141] and (**c**) TiN concentration increases the fracture toughness and hardness of the SiAlON/TiN composite [142]

composites was conducted in another study by Acikbas [84]. The significant increase in the wear rate of the composite reinforced with 17 wt% TiN was traced to the low fracture toughness of the sample.

Nekouee and Khosroshahi [49] employed the SPS method to produce fully dense β-SiAlON/TiN composites at 1750 °C, 30 MPa for 12 mins. The results demonstrated the existence of both the cubic TiN phase and the $Si_4Al_2O_2N_6$ phase within the matrix of the sintered composite. The addition of microsized TiO_2 as a precursor to the composite improved its mechanical properties, resulting in a fracture toughness of 6.3 MPa $m^{1/2}$ and a hardness of 14.6 GPa. The enhanced fracture toughness was noticed and ascribed to the toughening effect by the crack deflection mechanism. According to Smirnov et al. [50], β-Si_5AlON_7-TiN ceramic composites sintering with electric current assistance was also effective in achieving high relative densities (92% and higher) and improved mechanical properties. Using high-frequency induction sintering, the fracture toughness and Vickers hardness of the composite were found to increase with the addition of TiN, reaching values of 6.3 MPa $m^{1/2}$ and 12.6 GPa, respectively, for a composite containing 5 wt.% TiN. Using pulse electric current sintering, the composite containing 10% TiN has a Vickers hardness of 15.6 GPa and a fracture toughness of 8.3 MPa $m^{1/2}$. Therefore, the incorporation of titanium-based fillers can drastically increase the densification, hardness, and fracture toughness of SiAlON composite materials, making them suitable for high-performance applications.

β-SiAlON composites with Al_2O_3-C refractories

Different fillers, including aluminium oxide (Al_2O_3), have been used to modify the structure and properties of SiAlON in the literature [5, 56, 107, 109, 111, 143, 144]. Al_2O_3-C refractories are a type of advanced ceramic material used in high-temperature applications, such as furnace linings, burner nozzles, and heat exchangers. They are known for their excellent thermal stability, chemical resistance, and high melting point, making them suitable for use in harsh environments. The microstructure of β-SiAlON is profoundly impacted by Al_2O_3-C refractories. These refractories provide a framework for SiAlON formation through interactions between Si_3N_4, Al_2O_3, and carbon to improve their mechanical and thermal properties [145–147]. In a study by Yin et al. [111], they found that the addition of Al_2O_3 to β-SiAlON in Al_2O_3-C refractories improved the thermo-mechanical performance of the materials. It was observed that diverse morphologies of β-Sialon, such as a hexagonal prism, columnar, and plate-like structures, provide materials with high mechanical strength (Fig. 7a-c). The specimen with the plate-like β-SiAlON had a slightly

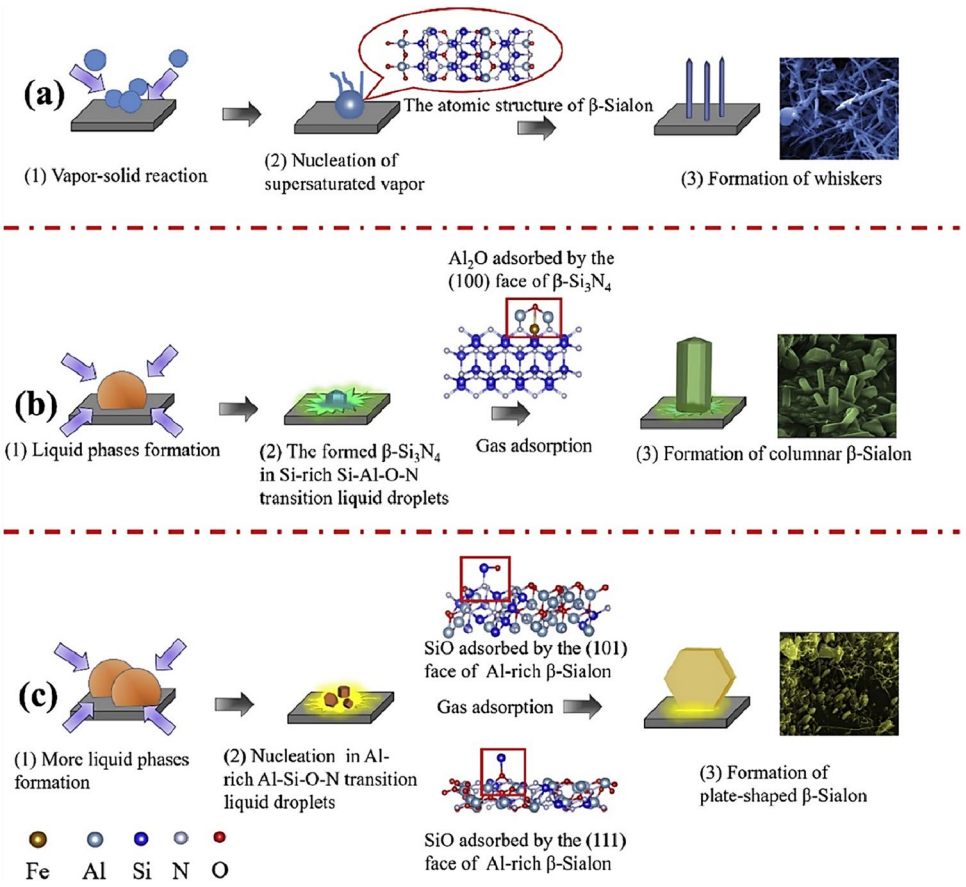

Fig. 7 (**a**-**c**) Growth processes of β-SiAlON with various morphologies. Copyright 2020 Elsevier [110]

greater cold modulus of rupture (CMOR) and cold crushing strength (CCS) compared to those with columnar and hexagonal prism structures, with highest values of 105.2 MPa for CCS and 27.2 MPa for CMOR, respectively. Moreover, the development of β-SiAlON resulted in strong thermal shock resistance, and the specimen with columnar β-SiAlON still had a residual strength ratio of 78% after five thermal shock cycles [110, 111]. Lan et al. [148] reported that the presence of Al_2O_3 significantly increased the hardness, density, and fracture toughness of SiAlON composites prepared by two-stage spark plasma sintering. The authors found that using Al_2O_3 as a filler in SiAlON composites leads to the production of completely dense ceramics with a density ranging between 3.22-3.24 g/cm^3. The inclusion of Al_2O_3 resulted in the formation of β-SiAlON with interlocking microstructures and corundum and silicon carbide phases. Improved hardness (15.68-15.95 GPa), and fracture toughness (6.38-7.03 MPa m$^{1/2}$) due to the presence of the hard phases within the microstructure of the developed composites were also reported. The introduction of Al_2O_3 was also found to increase SiAlON composites' thermal conductivity, with values ranging from 13.5-19.6 W/m-K [148]. According to Kovziridze et al. [149] and Deng et al. [143], the use of Al_2O_3 as a filler in SiAlON composites prepared by aluminothermic and nitro-aluminothermic processes leads to the formation of composites with improved corrosion resistance [5, 143]. Zhang and co-researcher [110] found that the utilization of Fe_2O_3 as a catalyst to Al_2O_3-C refractories resulted in the formation of β-SiAlON with a one- or two-dimensional shape, which significantly improved the CMOR and heat modulus of rupture (HMOR) of the developed materials by 45.07% and 60.47%, respectively. The findings of Yin et al. [109] and Zhang et al. [112] also revealed that the addition of Fe_2O_3 to Al_2O_3-C refractories resulted in the formation of plate-like β-Sialon, which improved the CMOR and CCS of the materials.

Sintering additives such as Sm_2O_3 and La_2O_3 also improve the sintering behaviour and densification of SiAlON composites. In a study on the preparation of SiC-SiAlON and Al_2O_3-SiAlON composites using alumothermal processes, the addition of Sm_2O_3 [29] and La_2O_3 [150] was found to make the density higher and hardness of the resulting composites. The addition of Sm_2O_3 resulted in a density increase of up to 4.1% and a hardness increase of up to 9.8% [29], while the addition of La_2O_3 resulted in a density increase of up to 5.5% and a hardness increase of up to 22.8% [150]. Hence, the structure and properties of SiAlON composites can be significantly influenced by using Al_2O_3 fillers, producing enhanced mechanical, thermal, and thermal shock resistant qualities. These properties can be

tailored by controlling the various parameters, including the type and amount of catalyst used, the Al_2O_3/Si_3N_4 ratio, and the sintering temperature.

β-SiAlON composites with metallic inclusions

Metallic inclusions such as Mg, Ti, Ca, and Fe are added to SiAlON composites to significantly influence their structure and properties and catalyze the reaction process [26, 40, 113, 120, 126, 151]. The addition of Mg has been shown to improve the IR transparency of SiAlON ceramics. Joshi et al. [40] fabricated IR Mg-α/β-SiAlON: Ba^{2+} ceramics by the hot pressing technique. Their results showed that $BaCO_3$ addition increases the α-SiAlON phase in the sintered bodies due to the extra liquid phase that permits Mg^{2+} migration in the α-Si_3N_4 lattice. According to the authors, this resulted in ceramics with a light transmission of about 78% in the IR region (2500 nm) and a hardness of 21.4 GPa [40]. Yurdakul and Turan used transmission electron microscopy to determine if it was possible to include Ti transition metal into the crystal structure of β-SiAlON in β-SiAlON-TiN composite material. [120]. The study demonstrated that Ti (transition metal) may penetrate the β-SiAlON crystal structure, creating Ti-doped SiAlON-based materials for different engineering applications. Ahmed et al. [122] studied the influence of particle size of α-SiAlON precursor and the amount of cubic boron nitride (cBN) reinforcement on the microstructure and mechanical properties of cBN-reinforced α -SiAlON composites fabricated using SPS at 1500 °C for 30 mins. The use of a ball milling technique with high energy was shown to cause a phase change from cBN to hBN, as well as an α-to β-Sialon phase change. The developed composites displayed greater mechanical strength than pristine SiAlON, with a Vickers hardness (HV10) value of up to 24.0 GPa as opposed to pure alpha SiAlON's 21.6 GPa. According to Adeniyi et al. [152], the addition of Ni to α-SiAlON ceramics enhanced the corrosion resistance and mechanical properties of the resulting composites. The authors achieved the α-SiAlON/Ni composites via SPS at 1500 °C for 30 min. It was found that the inclusion of Ni resulted in an improvement in the densification up to 15 wt% Ni, corrosion resistance, as well as an increase in the hardness and fracture toughness of the sintered composites. The improvement in mechanical properties was attributed to Ni particles' strengthening effect and the establishment of a Ni/SiAlON interpenetrating phase composite.

The addition of Fe-containing compound has been found to improve the mechanical characteristics and microstructure of β-Sialon ceramic. Sun et al. [126] demonstrated this by reinforcing β-SiAlON composites with Fe_3Al. The addition of Fe_3Al was found to improve the sinterability of the composites and resulted in an increase in the flexural strength and hardness of the composites. Furthermore, enhanced composites' resilience to wear was also reported. Zhang et al. [113] introduced Fe, Co and Ni transition metals to aid the catalytic reaction during the nitridation of β-SiAlON. The authors concluded that the addition of transition metals greatly improved the amount of vapour generated, which significantly enhanced the nitridation process of Si and eased β-SiAlON nanofibers formation. Also, the addition of molten Al as a heating medium in a fast heating thermal shock test (FHTST) for β-SiAlON has equally been demonstrated by Li et al. [26]. The authors stated that with a temperature differential (T) up to 900 °C, Vickers cracks did not spread in melted metal in the FHTST, and the retained strength did not diminish. However, when the temperature exceeded 600°C, the maintained strength for use with room temperature water in the quenching thermal shock test (QTST) dramatically decreased, and the indentation fractures substantially spread. The FEM calculation demonstrated that the variable stress state (compressive or tensile stress) on the surface might be the source of the discrepancies between the FHTST and QTST findings. The distribution of stress and temperature in the β-SiAlON specimens at 0.01 s for FHTST compared to the quench thermal shock test (QTST) is shown in Fig. 8a-c. They suggested that a useful thermal shock evaluation

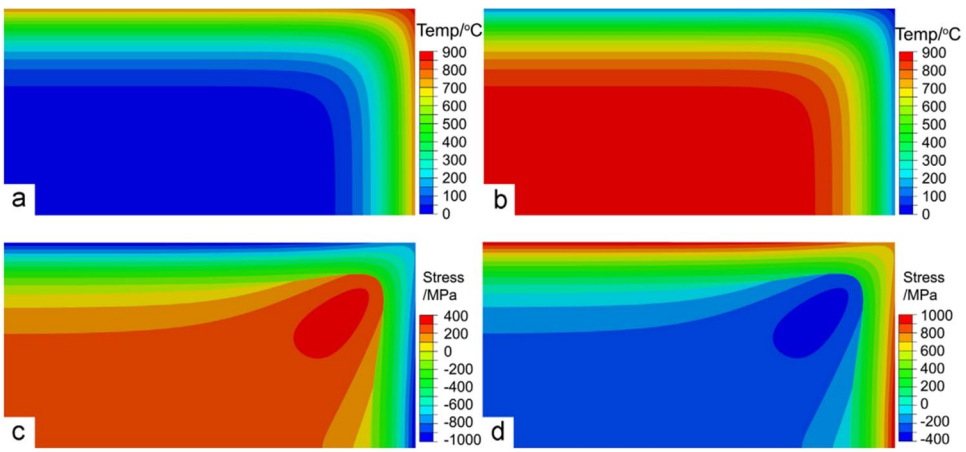

Fig. 8 Distribution of temperature and stress in the β-SiAlON specimens at 0.01 s: FHTST specimen temperature distribution, (**b**) QTST specimen temperature distribution, (**c**) FHTST specimen (molten Al) stress distribution, and (**d**) QTST specimen stress distribution. Copyright 2015 Elsevier [26]

technique for the ceramics utilized in the business of nonferrous metals would be FHTST with molten metal. In general, the incorporation of metallic components, such as Mg, Ti, Ca, and Fe can significantly impact the composition and characteristics of SiAlON composites, including their IR transparency, microstructure, mechanical properties, and wear resistance. Understanding these relationships can help in the design and optimization of SiAlON composites for specific applications.

α-phases SiAlON-based composites with Micro and Nano inclusions

α-SiAlON is a ceramic material with excellent hardness, high temperature stability, and good chemical resistance. It is extensively utilized in many different applications, such cutting tools, wear-resistant coatings, and ball bearings. It can be reinforced with various inclusions by combining α-SiAlON with other materials, such as cBN, hBN, Si_3N_4, Ca, SiC, Y_2O_3 (yttrium oxide), Ni, WC (tungsten carbide), and TiCN (titanium carbonitride). Several reports in the literature [6, 30, 38, 74, 103, 104, 114, 117, 123, 153–158] revealed that these inclusions can improve The α-SiAlON ceramics' mechanical characteristics and resistance to wear, as well as enhance their performance in various applications. The addition of cBN has been found to improve the hardness and fracture toughness of α-Sialon composites [38, 123, 153, 154]. In a study conducted by Gareth et al. [123] on α-SiAlON–cBN composites using FAST/SPS–sintering at 1575 °C -1625 °C, the hardness of the materials increased up to 21 GPa with the inclusion of 10 vol.% cBN, while with 30 vol. % cBN, the fracture toughness improved to over 8 MPa $m^{0.5}$. Due to the cBN grains' poor matrix bonding, crack deflection at those grains was thought to cause an increase in fracture toughness.

However, as the sintering temperature increased, the mechanical properties of these composites started to degrade because of the presence of hBN (hexagonal boron nitride) near the junction of cBN and the matrix. (Fig. 9a & b). In another related work by Gareth et al. [154], the influence of cBN grain size (10 µm and 100 µm) on the properties of SPS produced α-SiAlON ceramics at 1550 °C was studied. Conversion of cBN to hBN was reported on the surface of the smaller grain size, while transformation occurred both on the surface and at the internal grain boundaries inside the cBN grains of the larger grain size. The authors established that the higher the hBN formation, the higher the fracture toughness and the lower the final product's hardness. Hence, the properties of the composite ceramic reinforced with 100 µm cBN grain size are greatly influenced by the sintering temperature.

Similarly. the inclusion of hBN has also been found to affect the properties of α-SiAlON/BN composite ceramics. Shan et al. [38] examined the effect of hBN on the flexural strength of these ceramics. It was found that the inclusion of hBN contributed to the powder body's densification but had little effect on the phase transformation of α-SiAlON. The authors found that the highest flexural strength was obtained with 20 wt.% hBN and the formation of β-SiAlON was suggested as a significant explanation for the increased strength [153, 154]. The use of Y_2O_3 as a dopant has been found to improve the sinterability and mechanical properties of α-SiAlON ceramics. Choi et al. [127] examined the impact of Y_2O_3 on the microstructure and mechanical properties of α -SiAlON-based composite ceramics using a gas pressure sintering furnace at 1820 °C for 90 min under 1 MPa nitrogen. It was found that the addition of Y_2O_3 improved the sinterability and density of the ceramics and increased the fracture toughness but reduced hardness (Fig. 9c). The inclusion of Y_2O_3 further led to the creation of yttrium-containing oxide phases, which were suggested to act as a strengthening phase and improve the bonding between the grains.

Several authors [9, 30, 103, 104, 114, 117] have posited that the inclusion of SiC or WC in α-SiAlON significantly improves the tribo-mechanical properties of the resulting composites. SiC particles are typically present as micron-sized grains and form a homogenous distribution within the matrix. Kushan Akin et al. [117] synthesized α-SiAlON ceramic composites by adding SiC particles using SPS at 1500 °C for 30 min. The addition of SiC resulted in improved hardness and fracture toughness compared to monolithic α-SiAlON ceramics. The thermal diffusivity of α- and β-SiAlON ceramics was also improved by the addition of 0.25 wt% SiC. Liu et al. [30] studied the effects of temperature on the phase development, microstructures, and mechanical properties of SPSed (1800–2000 °C in an environment of 0.6 atm nitrogen) α-SiAlON composites reinforced with 80 wt% α-SiC. Their results showed that the addition of SiC enhanced flexural strength and fracture toughness and produced self-reinforcing microstructures. Biswas et al. [103] consolidated WC-reinforced α-SiAlON composites by SPS at 1750 °C, 40 MPa for 25 min. The authors reported that as the indentation load increases, the K_{IC} values of the pure α-SiAlON and 40 wt % WC/α-SiAlON composite increased, but those of the pure WC fluctuated within a narrow range of 4.16-4.50 MPa-$m^{0.5}$. This behaviour was attributed to the naturally brittle character and the equiaxed grain shape of WC. The changes in K_{IC} of the developed WC/α-SiAlON composites as a result of the indentation load are depicted in Fig. 9d.

Hence, the addition of nano- and micro-inclusions of cBN, hBN, Si_3N_4, Ca, SiC, WC, and TiCN significantly influence the tribomechanical attributes of the composite, like hardness, toughness, and wear resistance. However, the effect of these inclusions on the structure and properties of

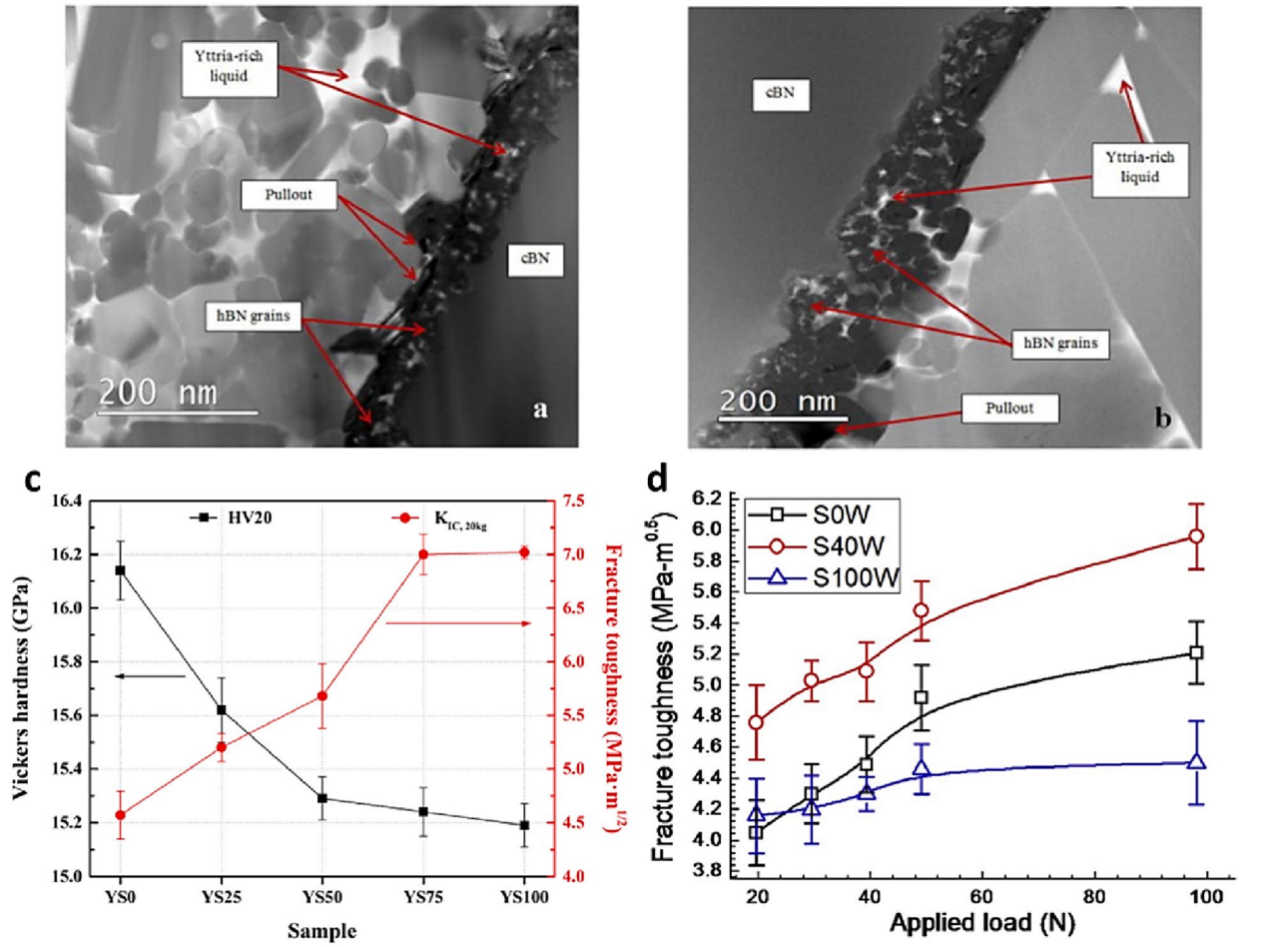

Fig. 9 STEM micrograph of M1025 sintered with 10% cBN at temperatures of (**a**) 1575°C and (**b**) 1625°C. It is believed that the hBN grains are breaking apart because of the poor wetting of hBN with the oxide-rich glassy phase. Copyright 2013 Elsevier [123] (**c**) Vickers IF technique measurements of hardness (HV20) and fracture toughness (K_{IC},20kg) as functions of Y_2O_3 additive content. Copyright 2022 Elsevier [127] (**d**) variations in the chosen specimens' fracture toughness (K_{IC}) under indentation stresses ranging from 2 to 10 Kgf. Copyright 2020 Elsevier [103]

the composite may vary depending on their concentration and distribution within the matrix.

O-, X-, and R-phases SiAlON-based composites with Micro and Nano inclusions

O-SiAlON composite is a type of ceramic material that is composed of silicon, aluminum, oxygen, and nitrogen. It is known for its high strength, high temperature resistance, and excellent corrosion resistance. The structure and composition of the O-SiAlON composite are closely related to its properties and can be tailored by incorporating various inclusions such as Si_3N_4, SiC, Al_2O_3, Gd_2O_3, Yb_2O_3, TiN, and TiO_2 [19, 32, 118, 155, 159, 160]. The X-phase of SiAlON composite materials has a crystal structure similar to that of mullite, with columns of octahedral aluminum oxide units bridged by tetrahedral units of aluminum oxide and silicon oxide. Its stoichiometry can vary from $SiAlO_2N$ to $Si_{16.9}Al_{22.7}O_{48.8}N_{11.6}$. Hot-pressed X-SiAlON composites containing 28% volume fraction of Al_2O_3 platelets have been found to possess a bulk density of 3.18 g/cm^3, a fracture toughness of 4.16 MPa m$^{0.5}$, and a hardness of 1270 kg/mm^2 [34]. Dayan et al. [159] produced an O-SiAlON composite in a ball milling process by combining silicon carbide fines, Si, Al, and alumina micro-powders having different activities. These micro-powders were then wet mixed with silicon carbide particles and a binder, shaped into specimens, and fired at a temperature of 1450 °C in a nitrogen atmosphere. The resulting O-SiAlON composite has a SiAlON content of up to 23.5%, a reduction in the amount of unreacted alumina and silicon nitride from 8.78 mass% to 1.79 mass%, and an increase in the percentage of micropores with sizes under 1 µm from 30% to 68%. The CO resistance of the O-SiAlON composite is also improved to level A.

Liu et al. [155] modified the structure and composition of the O-SiAlON composite by adding h-BN nanosheets as a reinforcement phase. Their results showed improvement in the mechanical and thermal properties, including the damage tolerance and toughness of the O-SiAlON composite. The thermal diffusivity and conductivity of the developed O-SiAlON composite significantly increased due to the ultra-high thermal conductivity of the h-BN nanosheets. Consequently, the O-SiAlON composite exhibits good thermal shock resistance, with a water absorption of only 14.4% and a residual strength ratio of 73% after 15 thermal cycles at a temperature difference of ΔT=1100 °C.

O-SiAlON composite can also be prepared by a repeated sintering method. Ma and Bao [116] investigated the oxidation behaviour of Si_3N_4/O′-SiAlON composite sintered in a furnace under 3 MPa N_2 gas pressure at 1,750 °C, 5 °C/min, for 2 h. The authors observed that repeated sintering resulted in an increasing fraction of the O′-SiAlON phase and densification of the composite, leading to improved oxidation resistance of the developed composite. A reduction in the thickness of the oxide layer on the O-SiAlON composite after oxidation at high temperatures of 1100-1500 °C for 30 h was also reported. In addition, when Si_3N_4/O′-SiAlON composite ceramics are oxidized at 1500 °C for 30 h, the oxidation weight gain is decreased by 43.3%, from 0.432 mg/cm^2 to 0.025 mg/cm^2, compared to the oxidation weight increase after one-time sintering [116, 160].

Further work conducted by Ma and Bao [160] showed that the structure and composition of the O-SiAlON composite can be modified by the SiO_2 particle size. It was found that increasing the size of SiO_2 particles leads to an increase in bulk density and bending strength, as well as a decrease in oxidation weight gain. However, at higher SiO_2 sizes, these properties may begin to decrease. The 3D morphology of composite ceramics made of Si_3N_4/O'-SiAlON with various SiO_2 contents and oxidized for 30 hours at 1500 °C is shown in Fig. 10i. A steady decrease in the distance between the highest and lowest peaks could be seen. To differentiate the phase of the oxidized surface of the sample, Fig. 10ii displays the oxidized surfaces of samples with 0 wt.% and 7.5 wt.% SiO_2 oxidized for 30 h at 1500 °C. The presence of equiaxed grains and dispersedly thin rod-like grains were observed on the sample's oxidized surface (Fig. 10ii(a) and (b)). Both were recognized by the EDS; the thin rod-like grains included Y, Si, and O elements, while the equiaxed grains had Si and O elements. In addition, the elements Al, N, O, Si, and Y were evenly dispersed on the oxidized surface according to the EDS mapping images of the analyzed samples. The authors reported that a composite with 2 µm SiO_2 grain size displayed a maximum bulk density of 2.86 g/cm^3, an ideal bending strength of 305.38 MPa, and an oxidation weight increase of 0.025 mg/cm^2.

In addition to the inclusions mentioned above, other factors can also affect the structure and composition of the O-SiAlON composite. For instance, the employed sintering temperature and time can impact the microstructure and densification of the composite, as well as its mechanical properties, for example, flexural strength and hardness, but may also result in the formation of defects or grain growth. The addition of a second phase, such as Al_2O_3 or SiC, can also influence the structure and properties of the O-SiAlON composite. According to Shao et al. [119], the addition of Al_2O_3 to O-SiAlON improves the composite's hardness and wear resistance, while Kaya et al. [118] found that the incorporation of SiC into O-SiAlON ceramic increases the resultant material's fracture toughness and flexural strength. The microstructure of O-SiAlON composite can also be influenced by the type and size of the silicon carbide particles used in its preparation. For instance, utilizing fine SiC particles leads to a more homogeneous microstructure and improved properties like hardness and flexural strength. On the other hand, using coarse SiC particles result in a more porous structure with lower mechanical properties [118, 124, 125].

The inclusion of TiN filler in O-SiAlON composite can affect its oxidation behaviour and phase compositions. Jiang et al. [121] subjected TiN/O′-Sialon ceramics to high-temperature oxidation of 1200 - 1300 °C in air. The oxidation of TiN and O′-Sialon was found to occur at approximately 500 °C and 1050 °C, respectively. The weight gain by the material dramatically rises along with increasing TiN concentration. Likewise, Yang et al. [128] used a selective oxidative process in the air at 800-1000 °C to produce in-situ TiO_2/O′-Sialon multiphase ceramics from TiN-reinforced O′-SiAlON composite ceramic material using a logarithm rule. According to the authors, in-situ TiO_2/O′-SiAlON multiphase ceramics cannot be made without an apparent activation energy of 56.1 kJ/mol. There is also no protective scale growth on the materials' surfaces. It was concluded that gas diffusion through the closed pore spaces is gradual and follows a rate-limiting step. Also, the addition of AlN to 27R-SiAlON polytype has been found to improve the densification, microstructure, and tribomechanical properties of the composite by Biswas et al. [94]. Sintering in the pulsed direct current mode (PM) was reported to produce better densification and wear resistance. Therefore, the structure and composition of the O-SiAlON composite can be tailored by incorporating various inclusions and manipulating sintering conditions, as well as the type and size of silicon carbide particles deployed. These modifications can significantly impact the mechanical, thermal, and corrosion resistance properties of the composite.

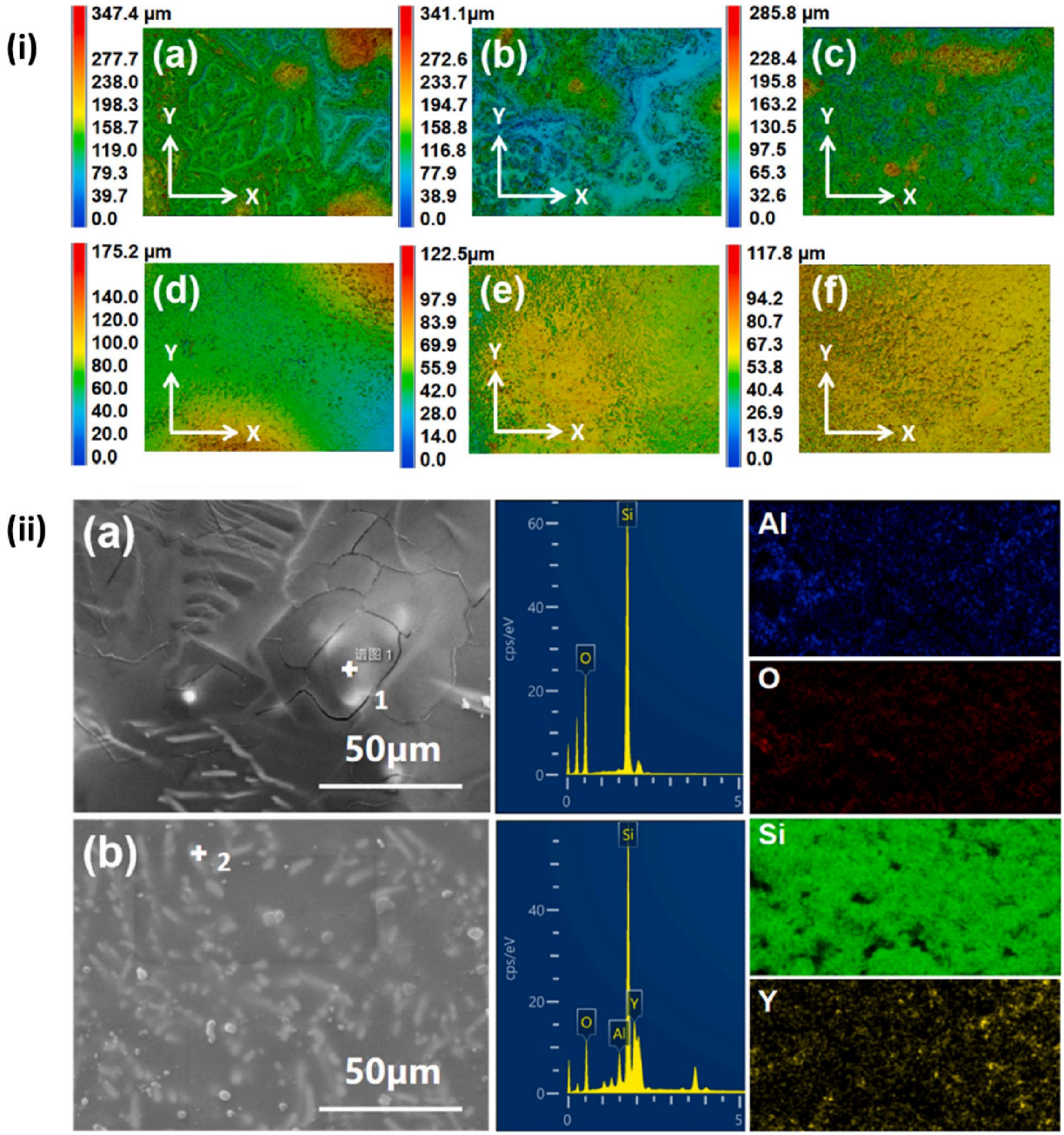

Fig. 10 (i) The Si_3N_4/O-SiAlON ceramics' 3D morphology after oxidizing with (**a**) 0 wt%, (**b**) 2.5 wt%, (**c**) 5 wt%, (**d**)7.5 wt%, (**e**) 10 wt%, (**f**) 12.5 wt%. (ii) EDS of the surface of the oxidized samples. Copyright 2021 Elsevier [116]

Application of SiAlON-based composites

Structural applications

SiAlON ceramics offer vast potential for use in structural and cutting applications, owing to their outstanding properties such as high-temperature stability, exceptional oxidation resistance, and impressive wear resistance. These properties make SiAlON ceramics suitable for usage as structural materials in high-temperature environments, as well as cutting tools for machining various materials [91, 115, 161, 162]. The use of SiAlON/TiN composite ceramic end mills for cutting nickel alloys is among the primary applications of SiAlON composite in structural applications. In a study by Grigoriev et al., Solid SiAlON/TiN ceramic end mills with DLC coating were developed for cutting nickel alloys, and their performance was evaluated. The results showed that the SiAlON/TiN ceramic end mills had excellent cutting

performance and wear resistance, making them suitable cutting tools and materials used in high-temperature environments. Some of the key steps in producing ceramic cutters are shown in Fig. 11 [163]. Zheng et al. investigated the cutting efficiency and wear mechanisms of SiAlON-Si3N4 graded nano-composite ceramic cutting tools produced via the hot-pressing technique, which can be utilized when cutting diverse materials [91, 115]. Their results showed that the ceramic cutting tools made of graded nano-composite SiAlON-Si_3N_4 had excellent cutting performance and low wear rates, making them suitable for use as cutting tools for machining various materials.

In addition to their use as cutting tools, SiAlON ceramics can also be used as structural materials in high-temperature environments. Zheng et al. [161] found that Sialon-Si_3N_4 graded ceramic tools had an excellent performance at high-speed machining, making them suitable for structural materials in high temperature environments. SiAlON ceramics can also be employed as building materials through the utilization of multiscale SiAlON ceramic composites with TiN reinforcement. Grigoriev et al. [164] showed that multiscale SiAlON ceramic composites with TiN reinforcement had excellent mechanical and tribological properties, making them appropriate for use as building materials in high temperature environments. Hence, SiAlON ceramics have a wide range of potential applications in structural and cutting applications due to their excellent features like high temperature stability, excellent oxidation resistance, and good wear resistance. These properties make SiAlON ceramics suitable as structural materials in high temperature environments, as well as for the machining of nickel alloys and tribological applications.

Coating and corrosion applications

Coating for corrosion prevention and control is important for various engineering applications. SiAlON composites have received much research on their potential usage in coating and corrosion applications because of their good characteristics, such as stability at high temperatures, excellent oxidation resistance, and good wear resistance. These properties make SiAlON ceramics suitable for application as protective coatings on various materials, including metals, alloys, and polymers. This section will cover a variety of coatings and corrosion applications of SiAlON composites, as well as the different synthesis methods and properties that make them suitable for these applications [87, 90, 164–168]. Modifying UV-curable coatings to increase their mechanical and hydrophobic qualities is one of the significant uses of SiAlON ceramics in coatings. In a study by Robakowska et al. [164], SiAlON and alumina were added to UV-curable coatings to improve their mechanical properties, hydrophobicity, and corrosion resistance. Both fillers were shown to be fully included in the examined matrix. The outcomes indicated that the inclusion of SiAlON and alumina significantly improved the mechanical properties, hydrophobicity, and corrosion resistance of the coatings. This is due to the high temperature stability and excellent SiAlON oxidation resistance, making it suitable for coating in high-temperature environments. Furthermore, images taken using an optical microscope demonstrate how the unfilled copolymer's fragmented structure reveals a level and homogenous surface (Fig. 12a). Meanwhile, according to AFM topography, the surface profile's amplitude is just about 30 nm (Fig. 12a). Figure 12b displays the viscosities of the compositions.

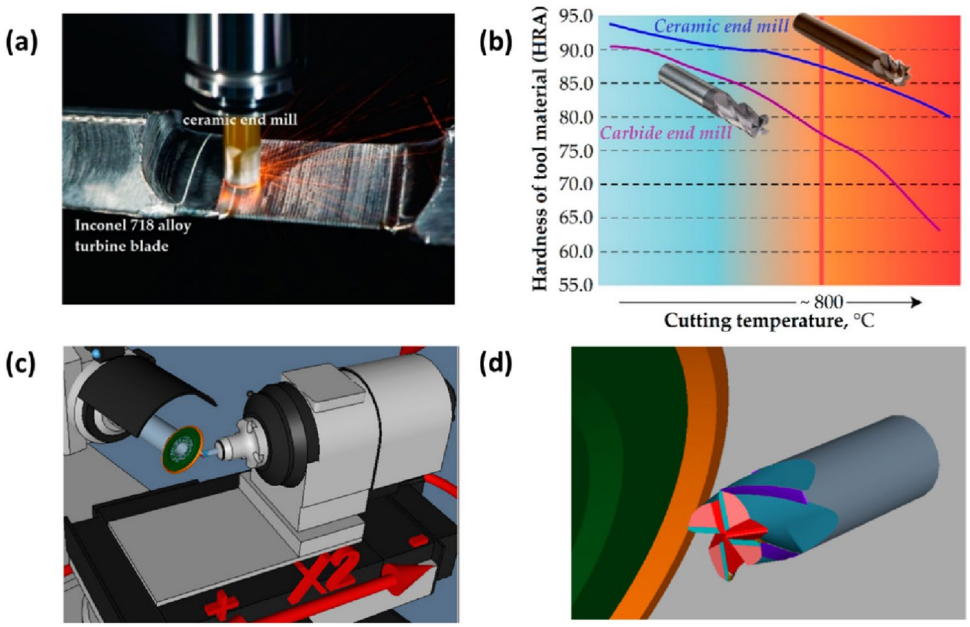

Fig. 11 (**a**) A nickel alloy turbine blade was milled at a high speed to demonstrate how SiAlON solid ceramic mills are used in industry. (**b**) the change in cutting temperature-dependent surface hardness of end mills made of hard alloy and ceramic. Solid ceramic end mill for diamond honing: (**c**) while creating a ceramic end mill, the relationship between the machine spindle and the workpiece; (**d**) cup-bevel wheel grinding of the secondary relief surface at the perimeter. Copyright 2021, MDPI [163]

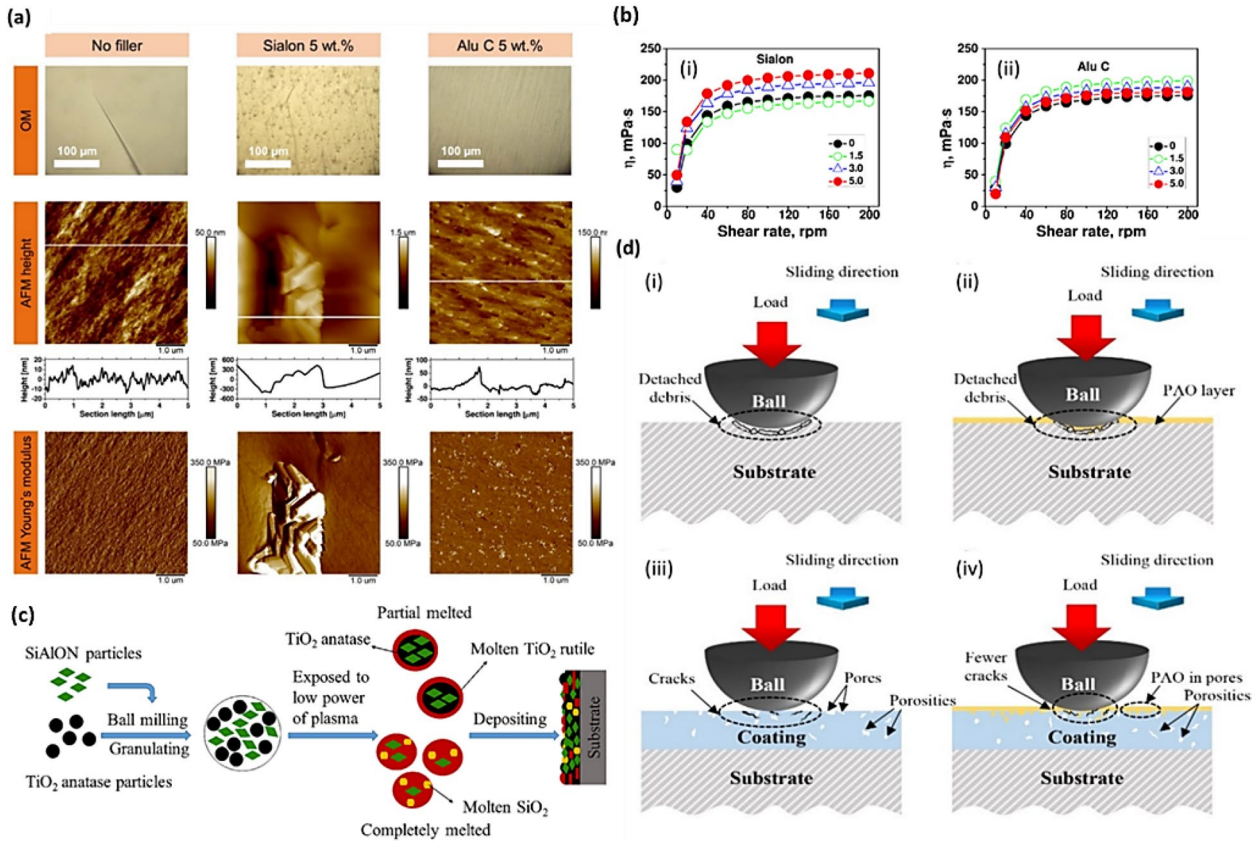

Fig. 12 (**a**) Cumulative OM and AFM images of control, filled with 5 wt % of Sialon and 5 wt % of Alu C particles on the bulk surfaces (fractured specimens). The cross-sectional analysis profiles are given behind the white lines in the height photos. Copyright 2021, MDPI. (**b**) How viscous the mixture is at 25 °C as a result of the filler concentration and shear rate; (i) Sialon, (ii) Alu C. Copyright 2021, MDPI [164]. (**c**) Illustrative representation of the TiO_2-SiAlON spray coating design. (**d**) Using poly-alpha-olefin (PAO) as a lubricant, the substrate and coating's ball-on-disc wear test in both dry and deprived lubricant circumstances; the following illustrations represent the wear mechanisms and system details: (i) S1, (ii) S2, (iii) C1, (iv) C2. Copyright 2021, MDPI [87]

SiAlON ceramics is also used as coatings on various materials through plasma spraying. Wang et al. [87] demonstrated this by producing TiO_2-SiAlON ceramic coatings by plasma spraying and studied their microstructure and wear behaviour. Their work showed that the TiO_2-SiAlON ceramic coatings had excellent wear resistance and low friction coefficient, making them suitable for wear-resistant coatings on various materials. As such, the wear processes depicted in Fig. 12c and d illustrate that under dry friction circumstances, wear debris builds up on the wear track and causes significant third-body abrasion as a result of the asperities of the Si_3N_4 ball's micro-cutting impact. The scientists discovered that the coating's minute pores can serve as reservoirs for lubrication to encourage fluid preservation at the contact zone. As a consequence, friction and wear rates are reduced and become more stable. Another vital application of SiAlON ceramic is in the corrosion protection of various materials. This was confirmed by the work of Moradi and colleagues [90, 165] on epoxy-sialon nanocomposite coatings prepared by electrostatic spraying. Their results showed that the epoxy-SiAlON nanocomposite coatings had excellent corrosion resistance, making them suitable for use as protective coatings on various materials.

Similarly, Sabagh and fellow scientists [169] examined how SiAlON nanoparticles affected the chemical and epoxy coatings' resilience against corrosion. Their findings demonstrated that the inclusion of SiAlON nanoparticles significantly improved the corrosion resistance of the epoxy coatings and their chemical resistance to various acids and bases. These authors attributed the performance of the nanocomposites to the excellent stability at elevated temperatures and good SiAlON oxidation resistance, making them resistant to corrosion in high temperature environments. Conclusively, SiAlON composites have a wide range of coating and corrosion uses due to their excellent attributes like a high temperature stability, excellent oxidation resistance, and good wear resistance. These properties make SiAlON ceramics suitable for use as protective coatings on various materials, including metals, alloys, and polymers. SiAlON composites can be synthesized through various methods for

coating, including solid-state reaction, spark plasma sintering, and pressureless sintering, depending on the desired microstructure and properties of the SiAlON composite. The electrostatic spraying method was found to be an effective way to produce coatings with improved corrosion resistance and mechanical properties. However, more investigation is required to completely understand the potential of SiAlON ceramics in coating and corrosion applications and to optimize their synthesis and processing for these applications.

Solar and LED applications

SiAlON composites have received much research on their potential use in solar and LED applications because of their superior mechanical and optical characteristics. These properties make SiAlON ceramics suitable for use as solar thermal storage materials and as phosphors in white LED applications [18–21, 129, 150]. In solar applications, SiAlON ceramics have been shown to have high thermal stability and good absorbance of solar radiation, making them suitable for use as solar thermal storage materials. For example, Liu et al. [19, 129] prepared O'-SiAlON/Si_3N_4 ceramics and their microstructure and performances were investigated for use in concentrated solar power applications. The results showed that the addition of Gd_2O_3 and Yb_2O_3 improved the microstructure and performance of the O'-SiAlON/Si_3N_4 ceramics, making them more suitable for use in concentrated solar power systems. In another study by According to Fu et al. [18], aluminothermic nitridation of coal-series kaolin was used to create in-situ synthesized SiAlON-Al_2O_3 ceramics for solar thermal storage. The outcomes revealed that the SiAlON-Al_2O_3 ceramics had good thermal stability and high absorbance of solar radiation, making them suitable for usage as solar thermal storage materials.

In LED applications, SiAlON ceramics have been used as phosphors to improve the colour rendering index of white LEDs. Zhang et al. [150] prepared Mg-doped SiAlON composites with La_2O_3 as an additive, and their optical and mechanical properties were looked into. Their findings indicated that the Mg-doped SiAlON composites had good optical and mechanical properties, consequently, they might be utilized as phosphors in white LED applications. Zinc phosphate glasses that were distributed with Eu-doped SiAlON were investigated for usage in white LED applications in another work by Zhang et al. [21]. The zinc phosphate glasses distributed with Eu-doped SiAlON have strong optical characteristics, according to their findings, making them acceptable for usage in white LED applications.

Similar to this, zinc borate glasses distributed with Eu-doped SiAlON were also investigated for usage in white LEDs in a work by Zhang et al. [20]. Figure 14 displays the samples of phosphor-in glass (PiG) made using zinc borate glass and SiAlON. The zinc borate glasses distributed with Eu-doped SiAlON reportedly showed good optical characteristics, according to the scientists. In light of this, they are utilized in white LED applications. The chromaticity of the x = 50 PiGs at varied concentrations of SiAlON is shown in Fig. 13a. Fig. 13b(i), (ii), and (iii) present the chromaticity of the composites that are 1-, 2-, and 3-mm thick, respectively. Given the same glass system and sample thickness, it can be shown that when SiAlON is raised, the color changes from blue to yellow. In summary, SiAlON ceramics have excellent optical and mechanical properties, enabling them to be utilized in solar and LED applications. Their use as solar thermal storage materials and as phosphors in white LED applications possess the capacity to improve the effectiveness and performance of these systems considerably.

Biomedical application

The biomedical application of SiAlON composites has gained significant attention due to their excellent properties, like high chemical stability, biocompatibility, bioactivity, and osteoconductivity. These properties make SiAlON composites suitable for use in a variety of biomedical applications, including bone repairing [22, 23, 82]. For instance, the β-SiAlON-Si_3N_4 composite ceramics have been shown by Li et al. [22] to have the potential for application in biological bacteriostasis (Fig. 14a and b). The growth of *E. coli* was shown to be suppressed by the composite ceramics, and the amount of β-SiAlON had an inverse relationship with the bacteriostatic effect. The release of chemical erosion, bacteriostatics, and ammonia nitrogen characteristics were proposed as the antibacterial mechanism, with the release of ammonia nitrogen limiting the development of E. coli, as seen in Fig. 14(a and b).

Similarly, Zhang et al. [23] investigated the potential using composite ceramic made of SiAlON and Si_3N_4 to heal bone. Their results showed that the developed SiAlON-Si_3N_4 composite ceramic displayed good mechanical properties and excellent biocompatibility, making it an appropriate material for bone repair. In addition, the SiAlON-Si_3N_4 composite ceramic had good bioactivity, which helps to promote the formation of new bone tissue. Figure 14c presents cell culture results using a ceramics composite made of SiAlON and Si_3N_4. Additionally, Wang et al. [82] investigated how ZrO_2 affected the biological and physicochemical characteristics of β-SiAlON-ZrO_2 composite ceramics. It was reported that the prepared β-SiAlON-ZrO_2 composite ceramics displayed improved corrosion resistance, mechanical properties, good biocompatibility, and cytocompatibility. Thus, making them an ideal candidate for drug delivery, tissue engineering and other biomedical applications. SiAlON-Al_2O_3 ceramics have also been studied for their potential use as biomaterials by Ye et al. [24]. The authors found that SiAlON-Al_2O_3 ceramics exhibited excellent

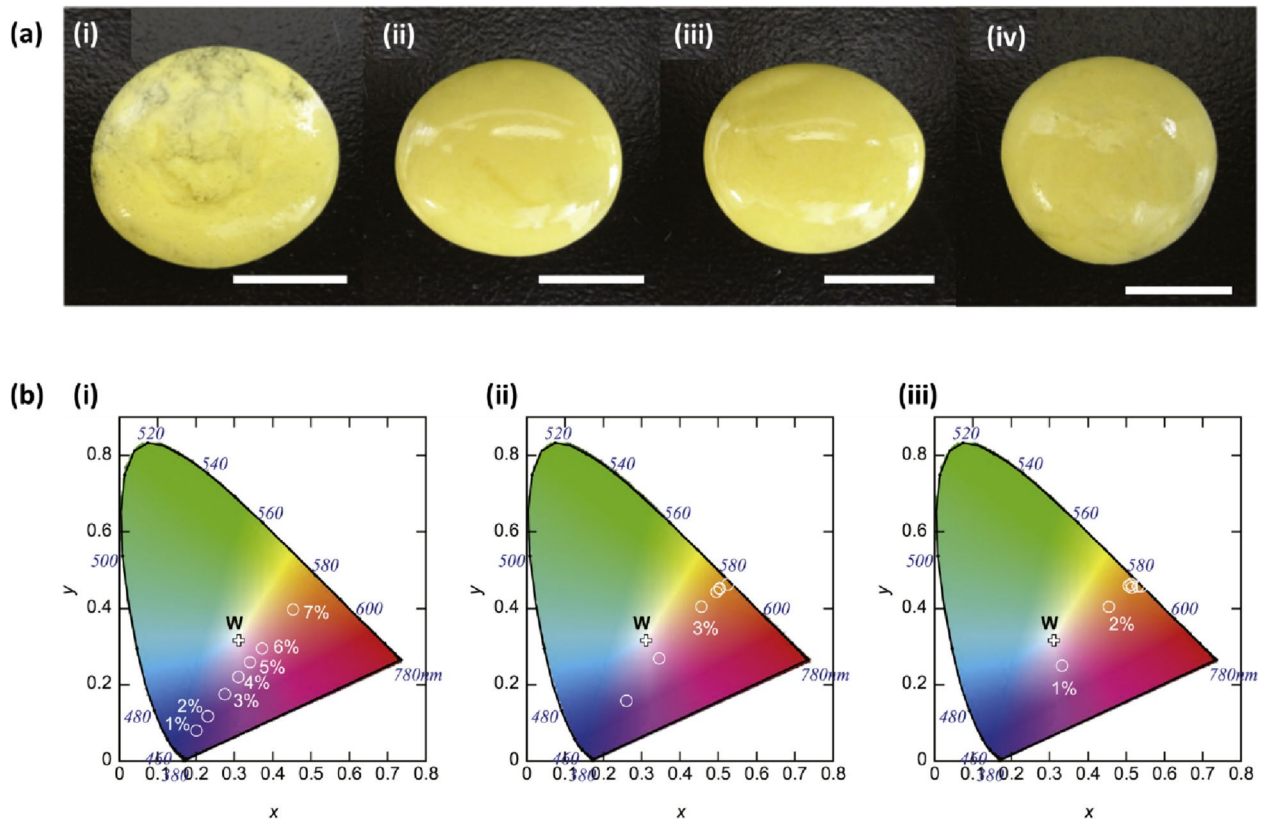

Fig. 13 (**a**) PiGs with 3 % mass of SiAlON are shown in the photos at x = 45 (i), 50 (ii), 55 (iii), and 60(iv), respectively. and (**b**) PiGs chromaticity diagram with x = 50 and thicknesses of (i) 1 mm, (ii) 2 mm, and (ii) 3 mm. Copyright 2018, Elsevier [20]

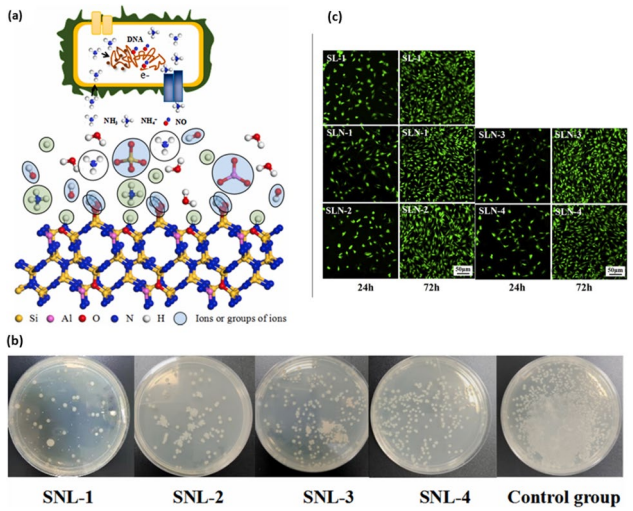

Fig. 14 (**a**) β-SiAlON-Si_3N_4 composite ceramic (sample SNL 1-4) hypothesized antibacterial mechanism. Copyright 2022, Elsevier [22]. (**b**) On the surface of the composite ceramic samples SNL 1-4 made of SiAlON, Si_3N_4, and Al_2O_3 in the control group, E. coli colonies developed. Copyright 2022, Elsevier [22]. (**c**) Results of the SiAlON-Si_3N_4 composite ceramics in cell culture. Copyright 2020, Elsevier [23]

biocompatibility appropriate for bone repair and drug delivery applications. The addition of Y_2O_3 has been reported to improve the physical characteristics and biocompatibility of ceramics made of β-SiAlON by Zhang et al. [25]. Therefore, the outcome of the works by several authors has established that β-SiAlON-Si_3N_4 composite ceramics possess good sintering properties, excellent biocompatibility, and bacteriostatic properties, which make them potential materials that are suited for biomedical applications including bone, drug delivery, and tissue engineering.

Filtration membrane application

Filtration membranes made from β-SiAlON ceramics have gained heightened visibility in recent years as a result of elevated temperature stability and excellent corrosion resistance. These properties make them suitable for the separation of oil-water emulsions, which are common in a variety of industrial processes [28, 170]. A novel design for β-SiAlON/graphene oxide ceramic membranes was created in a research by Kang et al. [28] for improved anti-fouling and separation of oil-water emulsions. The membranes were prepared by depositing graphene oxide onto β-SiAlON ceramic supports using a sol-gel method.

The resulting membranes showed improved water flux, anti-fouling performance, and oil droplet rejection compared to unmodified β-SiAlON membranes. Figure 15a illustrates the SiAlON/Graphene oxide nanocomposite membrane water/oil separation system. The authors attributed the improved performance to the super-hydrophilic nature of the graphene oxide-coated β-SiAlON membranes, which reduced oil adhesion and enhanced the separation of oil droplets. In a different study reported by Zhang et al. [170], β-SiAlON ceramic membranes with SiO_2 nanoparticles were modified to improve their separation performance in oil-water emulsion filtration. It was found that the modified membranes showed a high rejection rate of oil droplets, 4.5 µm in size on average, and good water permeability. Figure 15(b, c and d) displays the Permeation flux for varying flow velocities applied pressures during the operation and during an antifouling test. The authors attributed the improved performance to the surface modification of the β-SiAlON ceramic with SiO_2 nanoparticles, which increased the hydrophilicity of the membrane and reduced oil adhesion. Generally, the use of β-SiAlON ceramic in oil-water emulsion separation membranes has shown promising results, with the addition of SiO_2 nanoparticles and graphene oxide coating improving the separation performance of the membranes. Further research is needed to optimize the design and fabrication of these membranes for practical applications in industrial processes.

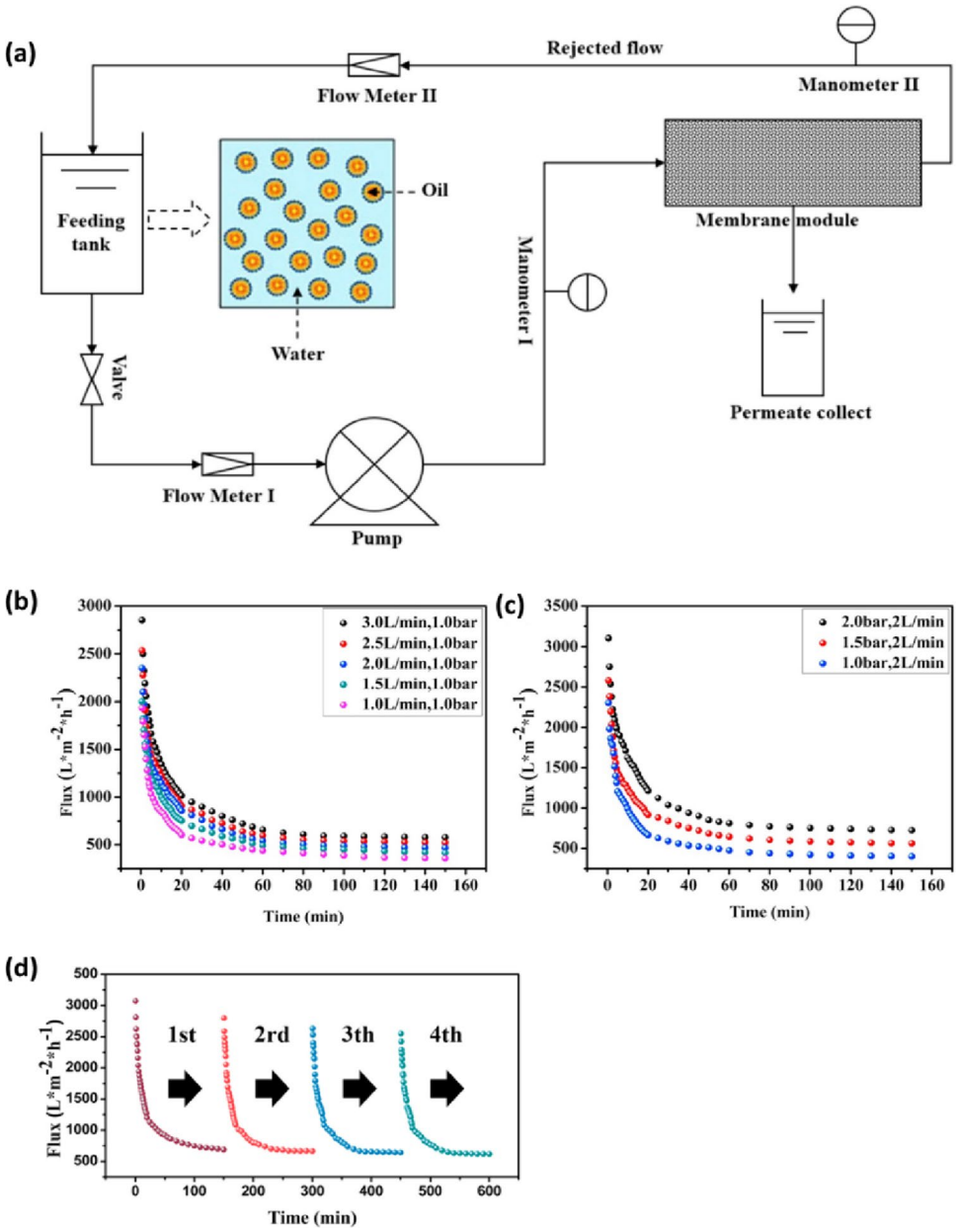

Fig. 15 (**a**) Illustration of SiAlON/Graphene oxide nanocomposite membrane water/oil separation system. Copyright 2019, Elsevier [28] Permeation flux for varying (**b**) flow velocities and (**c**) applied pressures during the operation. and (**d**) during an antifouling test. Copyright 2019, Elsevier [170]

Future research directions and challenges in SiAlON composites

The future of SiAlON composites research presents exciting avenues for advancement and innovation, alongside notable challenges to overcome. Advanced processing techniques offer promise in enhancing densification and microstructural control during sintering, necessitating exploration into methods such as spark plasma sintering (SPS) and hot isostatic pressing (HIP) [171]. Challenges include ensuring uniform grain growth and phase stability. Tailoring SiAlON phases for specific applications is another area ripe for exploration, requiring a deep understanding of phase transitions, crystallography, and stability [172]. Inclusion engineering offers opportunities to optimize the effects of metallic and non-metallic inclusions, but challenges remain in achieving uniform dispersion. Thermal conductivity enhancement, crucial for high-temperature applications, may be achieved through hybrid inclusions, although addressing anisotropic conductivity remains a hurdle. Improving fracture toughness involves controlling grain boundaries and microcrack interactions, with a focus on toughening mechanisms. Additionally, research into high-temperature oxidation resistance, multifunctional composites, industrial scale-up, environmental impact, and interdisciplinary collaboration will drive progress in SiAlON composites, paving the way for their widespread application across various industries [173–175].

Conclusion and future prospect

In this comprehensive review, we have explored the structure-property relationship and emerging applications of nano- and micro-sized fillers reinforced SiAlON composites. Through an extensive analysis of the literature, we have highlighted the versatility and potential of SiAlON composites in various fields. The structure-property relationship of SiAlON composites was thoroughly examined, revealing the critical role played by nano- and micro-sized fillers in enhancing their mechanical, tribological, and thermal properties. We discussed how the incorporation of fillers, such as metallic, ceramic, and nanocarbon materials, can tailor the properties of SiAlON composites for specific applications. Notably, the importance of β-SiAlON composites was underscored due to their superior mechanical strength and hardness, particularly when compared to other phases. Moreover, we emphasized the diverse range of potential applications for SiAlON composites with micro and nano-sized fillers. These applications span across various industries, including aerospace, electronics, automotive, and biomedical fields. SiAlON composites have shown promise in structural materials, cutting tools, coatings, corrosion protection, solar cells, LEDs, biomedical devices, and filtration membranes. More importantly, a new class of SiAlON composites with distinctive properties will become possible due to uncharted fabrication techniques like advanced additive manufacturing (3D and 4D printing). Hence, this review provides valuable insights into the fabrication, and utilization of SiAlON composites with enhanced properties. By elucidating the structure-property relationship and showcasing emerging applications, this article serves as a guide for researchers and engineers aiming to harness the full potential of SiAlON-based materials in sophisticated and exploratory applications. Further research in this area will undoubtedly lead to the development of even more advanced SiAlON composites with tailored properties to meet the demands of diverse industrial sectors.

Acknowledgements The Department of Mechanical and Mechatronics Engineering at the Tshwane University of Technology in Pretoria, South Africa, as well as the Faculty of Engineering and the Built Environment all provided financial assistance for this study, which the authors gratefully thank.

Author's contributions Olugbenga Ogunbiyi: Writing-original draft, Methodology, editing; Tamba Jamiru: Writing-review and editing; Gbolahan Joseph Adekoya: Writing-review and editing; Azeez Lawan Rominiyi: Writing-review and editing.

Funding Open access funding provided by Tshwane University of Technology.

Declarations

Conflict of interest The authors declare no conflict of interest.

Open Access This article is licensed under a Creative Commons Attribution 4.0 International License, which permits use, sharing, adaptation, distribution and reproduction in any medium or format, as long as you give appropriate credit to the original author(s) and the source, provide a link to the Creative Commons licence, and indicate if changes were made. The images or other third party material in this article are included in the article's Creative Commons licence, unless indicated otherwise in a credit line to the material. If material is not included in the article's Creative Commons licence and your intended use is not permitted by statutory regulation or exceeds the permitted use, you will need to obtain permission directly from the copyright holder. To view a copy of this licence, visit http://creativecommons.org/licenses/by/4.0/.

References

1. Canarslan, Ö.S., Koroglu, L., Ayas, E., Canarslan, N.S., Kara, A., Veronesi, P.: Susceptor-assisted fast microwave sintering of TiN reinforced SiAlON composites in a single mode cavity. Ceram. Int. **47**(1), 828–835 (2021). https://doi.org/10.1016/j.ceramint.2020.08.194

2. Valdes, A.F., et al.: Effect of MgAl2O4 on the growth of β–Si3Al3O3N5 prepared by carbothermal reduction by nitriding. Ceramics–Silikáty. **64**(3), 271–277 (2020)
3. Ahmed, B.A., Hakeem, A.S., Laoui, T., Al Malki, M., Ehsan, M.A., Ali, S.: Low-temperature spark plasma sintering of calcium stabilized alpha sialon using nano-size aluminum nitride precursor. Int. J. Refract. Met. Hard Mater. **71**, 301–306 (2018)
4. Yin, L., Jones, M.I.: Fabrication and properties of Sialon-ZrN composites by two-step sintering. Int. J. Refract. Met. Hard Mater. **92**, 105292 (2020). https://doi.org/10.1016/j.ijrmhm.2020.105292
5. Kovziridze, Z., et al.: Preparation of composites by nitro aluminothermic processes, over β–SiAlON matrix in the SiAlON-SiC-Al 2 O 3 system. Journal of Electronics Cooling and Thermal Control. **6**(02), 62 (2016)
6. S. S. Himanshu, R. Halder, M. Biswas, S. Bandyopadhyay, and M. F. Wani, "SPS Processed TiB_2 Reinforced Y-α-SiAlON Composites: High Temperature Tribomechanical Properties."
7. Bandyopadhyay, S.: The in situ formation of Sialon composite phases. J. Eur. Ceram. Soc. **17**(7), 929–934 (1997)
8. Sevgi Canarslan, Ö., Rosa, R., Köroğlu, L., Ayas, E., Kara, A., Veronesi, P.: Microwave sintering of SiAlON ceramics with TiN addition. Materials. **12**(8), 1345 (2019)
9. Kalyanwat, A.S., Sarkar, S., Biswas, M., Halder, R., Bandyopadhyay, S., Wani, M.: Spark plasma-sintered MoSi2-reinforced Y− α− SiAlON ceramics: mechanical and high temperature tribological properties. J. Aust. Ceram. Soc. **56**(1), 265–272 (2020)
10. Nguyen, T.P., et al.: Influence of SiAlON addition on the microstructure development of hot-pressed ZrB2–SiC composites. Ceram. Int. **46**(11, Part B), 19209–19216 (2020). https://doi.org/10.1016/j.ceramint.2020.04.258
11. Biswas, M., Sarkar, S., Bandyopadhyay, S.: Improvements in mechanical properties of SPS processed 15R-SiAlON polytype through structurally survived MWCNT reinforcement. Mater. Chem. Phys. **222**, 75–80 (2019). https://doi.org/10.1016/j.matchemphys.2018.09.084
12. Baskut, S., Sert, A., Çelik, O.N., Turan, S.: Anisotropic mechanical and tribological properties of SiAlON matrix composites containing different types of GNPs. J. Eur. Ceram. Soc. **41**(3), 1878–1890 (2021). https://doi.org/10.1016/j.jeurceramsoc.2020.10.071
13. Yang, H., Chang, M., Wang, H.J., Yao, Z.P.: Preparation of NiCr-Sialon-CaF2 Self-Lubricating Die Material and Its Friction at High Temperature. Trans. Tech. Publ. **279**, 167–171 (2018)
14. Baskut, S., Turan, S.: The effect of different GNPs addition on the electrical conductivities and percolation thresholds of the SiAlON matrix composites. J. Eur. Ceram. Soc. **40**(4), 1159–1167 (2020)
15. Cinar, A., Baskut, S., Seyhan, A.T., Turan, S.: Tailoring the properties of spark plasma sintered SiAlON containing graphene nanoplatelets by using different exfoliation and size reduction techniques: Anisotropic mechanical and thermal properties. J. Eur. Ceram. Soc. **38**(4), 1299–1310 (2018). https://doi.org/10.1016/j.jeurceramsoc.2017.10.004
16. Zheng, G., Zhao, J., Jia, C., Tian, X., Dong, Y., Zhou, Y.: Thermal shock and thermal fatigue resistance of Sialon–Si3N4 graded composite ceramic materials. Int. J. Refract. Met. Hard Mater. **35**, 55–61 (2012)
17. Yang, Z., et al.: Densification behavior, microstructure, mechanical and optical properties of Mg-doped sialon with fluoride additives. J. Eur. Ceram. Soc. **37**(5), 1985–1992 (2017)
18. Lao, X., et al.: In-situ synthesis of nitride whiskers-bonded SiAlON–Al2O3 ceramics for solar thermal storage by aluminothermic nitridation of coal-series kaolin. Ceram. Int. **48**(7), 10227–10235 (2022). https://doi.org/10.1016/j.ceramint.2021.12.236
19. Wu, J., Ding, C., Xu, X., Mi, K.: Effects of Gd2O3 and Yb2O3 on the microstructure and performances of O'-Sialon/Si3N4 ceramics for concentrated solar power. Ceram. Int. **47**(4), 5054–5060 (2021). https://doi.org/10.1016/j.ceramint.2020.10.083
20. Segawa, H., Hirosaki, N.: Optical properties of zinc borate glasses dispersed with Eu-doped SiAlON for white LED applications. Ceram. Int. **44**(5), 4783–4788 (2018)
21. Segawa, H., Hirosaki, N., Ohki, S., Deguchi, K., Shimizu, T.: Exploration of zinc phosphate glasses dispersed with Eu-doped SiAlON for white LED applications. Opt. Mater. **35**(12), 2677–2684 (2013). https://doi.org/10.1016/j.optmat.2013.08.006
22. Li, L., et al.: Effect of β-SiAlON content on the sintering and bacteriostatic properties of β-SiAlON–Si3N4 composite ceramics. Ceram. Int. (2022). https://doi.org/10.1016/j.ceramint.2022.07.316
23. Zhang, L., et al.: Feasibility of SiAlON–Si3N4 composite ceramic as a potential bone repairing material. Ceram. Int. **46**(2), 1760–1765 (2020)
24. Xie, H., Zhang, L., Xu, E., Yuan, H., Zhao, F., Gao, J.: SiAlON–Al2O3 ceramics as potential biomaterials. Ceram. Int. **45**(14), 16809–16813 (2019)
25. Li, M., et al.: Effect of Y2O3 on the physical properties and biocompatibility of β–SiAlON ceramics. Ceram. Int. **46**(15), 23427–23432 (2020). https://doi.org/10.1016/j.ceramint.2020.06.112
26. Li, Y., Yu, H., Jin, H., Shi, Z., Qiao, G., Jin, Z.: Fast heating thermal shock test for β-SiAlON with molten metals as heating medium. Ceram. Int. **41**(4), 6117–6121 (2015)
27. Li, Y., Ge, B., Wu, Z., Xiao, G., Shi, Z., Jin, Z.: Effects of h-BN on mechanical properties of reaction bonded β-SiAlON/h-BN composites. J. Alloys Compd. **703**, 180–187 (2017)
28. Kang, L., Zhao, L., Yao, S., Duan, C.: A new architecture of super-hydrophilic β-SiAlON/graphene oxide ceramic membrane for enhanced anti-fouling and separation of water/oil emulsion. Ceram. Int. **45**(13), 16717–16721 (2019)
29. Li, Y., Liu, D., Zeng, C., Shi, Z., Jin, Z.: Effects of Sm 2 O 3 Content on the Microstructure and Mechanical Properties of Post-Sintered Reaction-Bonded β-SiAlON. J. Mater. Eng. Perform. **25**, 1143–1149 (2016)
30. Liu, L., Ye, F., He, X., Zhou, Y.: Synthesis of α-SiC/α-SiAlON composites by spark plasma sintering: Phase formation and microstructures development. J. Eur. Ceram. Soc. **31**(12), 2129–2135 (2011). https://doi.org/10.1016/j.jeurceramsoc.2011.05.013
31. Li, Q., et al.: Effect of the starting AlN content on the phase formation and property of the novel in-situ fabricated X-SiAlON/BN composites. J. Eur. Ceram. Soc. **39**(4), 934–943 (2019). https://doi.org/10.1016/j.jeurceramsoc.2018.12.035
32. Ma, H., Bao, C.: Improved oxidation resistance properties of Si3N4/O'-SiAlON composite ceramics by a repeated sintering method. Int. J. Appl. Ceram. Technol. **19**(5), 2905–2915 (2022)
33. Nie, X., Li, Y., Jiang, P., Qin, H.: Formation mechanism of Sialon in alumina-ferro-silicon-nitride composite under nitrogen atmosphere at high temperatures. Solid State Sci. **86**, 19–23 (2018)
34. El-Amir, A.A.M., El-Maddah, A.A., Ewais, E.M.M., El-Sheikh, S.M., Bayoumi, I.M.I., Ahmed, Y.M.Z.: Sialon from synthesis to applications: an overview. J. Asian Ceramic Soc. **9**(4), 1390–1418 (2021). https://doi.org/10.1080/21870764.2021.1987613
35. Bake, A., et al.: Effect of nano-and micro-sized Si3N4 powder on phase formation, microstructure and properties of β′-SiAlON prepared by spark plasma sintering. Ceram. Int. **48**(2), 1916–1925 (2022)
36. Qin, H., Li, Y., Long, M., Nie, X., Jiang, P., Xue, W.: In situ synthesis mechanism of 15R–SiAlON reinforced Al2O3 refractories by Fe–Si liquid phase sintering. J. Am. Ceram. Soc. **101**(5), 1870–1879 (2018)

37. Shahedi Asl, M., Nayebi, B., Ahmadi, Z., Pirmohammadi, P., Ghassemi Kakroudi, M.: Fractographical characterization of hot pressed and pressureless sintered SiAlON-doped ZrB2–SiC composites. Mater. Charact. **102**, 137–145 (2015). https://doi.org/10.1016/j.matchar.2015.03.002
38. Shan, Y.C., Wang, G., Ye, H., Han, X.G., Xu, J.J., Li, J.T.: Fabrication of high strength α-SiAlON/BN composition ceramics by hot pressing. Key Eng Mater. **512-515**, 816–819 (2012)
39. Joshi, B., Lee, H.H., Kim, Y.H., Fu, Z., Niihara, K., Lee, S.W.: Hot pressed translucent (Mg, Y)-α/β-Sialon ceramics. Mater. Lett. **80**, 178–180 (2012)
40. Joshi, B., Li, B., Kshetri, Y.K., Wang, H., Wohn Lee, S.: IR transparent hot pressed Mg-α/β-Sialon:Ba2+ ceramics. Ceram. Int. **40**(8, Part B), 13041–13047 (2014). https://doi.org/10.1016/j.ceramint.2014.05.001
41. Hong, D., Yin, Z., Guo, F., Yuan, J.: Microwave synthesis of duplex α/β-SiAlON ceramic cutting inserts: Modifying m, n, z values, synthesis temperature, and excess Y2O3 synthesis additive. J. Adv. Ceram. **11**(4), 589–602 (2022)
42. Chockalingam, S., Traver, H.K.: Microwave sintering of β-SiAlON–ZrO2 composites. Mater. Des. **31**(8), 3641–3646 (2010)
43. Yeung, K.-W., et al.: Fabrication of ceramic bioscaffolds from fly ash cenosphere by susceptor-assisted microwave sintering. J. Eur. Ceram. Soc. **42**(10), 4410–4419 (2022)
44. Egorov, S.V., et al.: Rapid sintering of barium titanate ceramics using direct and susceptor-assisted microwave heating. Materialia. **24**, 101513 (2022)
45. Letwaba, J., Tlhabadira, I., Daniyan, I., Daramola, O., Sadiku, R., Seerane, M.: Development and preliminary process design of beta-SiAlONs by the spark plasma sintering process. Int. J. Adv. Manuf. Technol. **109**(9), 2603–2613 (2020)
46. Hotta, M., Goto, T.: Spark Plasma Sintering of βSiAlON-cBN Composite. Mater. Sci. Forum. **561-565**, 599–602 (2007). https://doi.org/10.4028/www.scientific.net/MSF.561-565.599
47. Ye, F., Hou, Z., Zhang, H., Liu, L., Zhou, Y.: Spark plasma sintering of cBN/β-SiAlON composites. Mater. Sci. Eng. A. **527**(18), 4723–4726 (2010). https://doi.org/10.1016/j.msea.2010.04.034
48. Luo, J., et al.: Superplastic forging for sialon-based nanocomposite at ultralow temperature in the electric field. Sci. Rep. **9**(1), 1–6 (2019)
49. Nekouee, K.A., Khosroshahi, R.A.: Sintering behavior and mechanical properties of spark plasma sintered β–SiAlON/TiN nanocomposites. Int. J. Refract. Met. Hard Mater. **61**, 6–12 (2016). https://doi.org/10.1016/j.ijrmhm.2016.08.002
50. Smirnov, K.L., Grigoryev, E.G., Nefedova, E.V.: SiAlON-TiN Ceramic Composites by Electric Current Assisted Sintering. Mater. Sci. Forum. **946**, 53–57 (2019). https://doi.org/10.4028/www.scientific.net/MSF.946.53
51. Yin, L., Gao, W., Jones, M.I.: Wear behaviour and electrical conductivity of β-Sialon-ZrN composites fabricated by reaction bonding and gas pressure sintering process. Ceram. Int. **45**(2, Part A), 2266–2274 (2019). https://doi.org/10.1016/j.ceramint.2018.10.140
52. Yin, L., Jones, M.I.: Effect of Applied Pressure on Densification and Mechanical Properties of Sialon-ZrN Composites Fabricated Through a Reaction Bonding / Gas Pressure Sintering Process. IOP Conf. Series: Mat. Sci. and Eng. **389**, 012021 (2018). https://doi.org/10.1088/1757-899x/389/1/012021
53. Li, J.Q., et al.: High mechanical properties of β-SiAlON/TiC0.3N0.7 ceramic composite prepared by pressureless spark plasma sintering. J. Asian Ceramic Soc. **9**(1), 393–403 (2021). https://doi.org/10.1080/21870764.2021.1874642
54. Ma, B., Gao, Z., Su, C., Ren, X., Li, G., Zhu, Q.: Recycling of coal ash for production of dense β-Sialon/ZrN/ZrON-based ceramics without sintering aids via pressureless sintering. Int. J. Appl. Ceram. Technol. **17**(1), 175–183 (2020)
55. Mapoli, T.O., Mutombo, K., Annan, K.A., Siyasiya, C.W.: Microstructures and Phases Analysis of the 60Al-40V Master Alloy Produced by the Aluminothermic Process. Metallograph. Microstruct. Anal. **11**(3), 405–414 (2022)
56. Kovziridze, Z., et al.: Obtaining of Nanocomposites in SiC-SiAlON and Al 2 O 3-SiAlON System by Alumothermal Processes. J. Electron. Cool. Thermal. Control. **4**(04), 105 (2014)
57. Arik, H.: Synthesis of Si3N4 by the carbo-thermal reduction and nitridation of diatomite. J. Eur. Ceram. Soc. **23**(12), 2005–2014 (2003)
58. Yin, Q., et al.: Mechanism and experimental study on preparation of high-quality vanadium nitride by one-step vacuum carbothermal reduction nitridation method. Vacuum. 111672 (2022)
59. Tian, X., Su, K., Ouyang, D., Gao, J., Jia, Q., Liu, X.: Effect of impurities of Fe2O3 and TiO2 in bauxite on oxidation kinetics of β-SiAlON powders. Corros. Sci. **203**, 110374 (2022)
60. Qiu, J.Y., Tatami, J., Zhang, C., Komeya, K., Meguro, T., Cheng, Y.B.: Influence of starting material composition and carbon content on the preparation of Mg-α SiAlON powders by carbothermal reduction-nitridation. J. Eur. Ceram. Soc. **22**(16), 2989–2996 (2002)
61. Chung, C.-C., Jean, J.-H.: Synthesis of Ca-α-SiAlON: Eux phosphor powder by carbothermal-reduction–nitridation process. Mater. Chem. Phys. **123**(1), 13–15 (2010)
62. Yamamoto, O., Ishida, M., Saitoh, Y., Sasamoto, T., Shimada, S.: Influence of Mg2+ on the formation of β-SiAlON by the carbothermal reduction-nitridation of homogeneous gel. Int. J. Inorg. Mater. **3**(7), 715–719 (2001)
63. Li, Y., et al.: Synthesis of ZrN–sialon composites from zircon and alumina by carbothermal reduction–nitridation. Mater. Res. Bull. **47**(11), 3273–3276 (2012)
64. Lv, Z., et al.: Growth mechanism and synchronous synthesis of 1D β-sialon nanostructures and β-sialon-Si3N4 composite powders by a process of reduction nitridation. Mater. Res. Express. **6**(6), 065054 (2019)
65. Wu, J., Jiang, T., Xue, X.: Effect of α-Si_3N_4 Addition on Sintering of α-Sialon Powder via Carbonthermal Reduction Nitridation of Boron-rich Slag-based Mixture. IOP Conf. Series: Mat. Sci. and Eng. **18**(20), 202018 (2011). https://doi.org/10.1088/1757-899x/18/20/202018
66. Xiangcheng, L.I.: Study on Preparation and Reaction Mechanism of B4C/β-Sialon/SiC/Al 2O3 Composite Powder. In: Advances in Machinery, Materials Science and Engineering Application: Proceedings of the 8th International Conference on Advances in Machinery, Materials Science and Engineering Application (MMSE 2022), vol. 24, p. 203. IOS Press (2022)
67. Xue, L., et al.: Microstructure and ablation behavior of C/C–HfC composites prepared by precursor infiltration and pyrolysis. Corros. Sci. **94**, 165–170 (2015)
68. Liu, C.-X., Chen, J.-X., Su, Z.-A., Xin, Y., Cao, L.-X., Huang, Q.-Z.: Pyrolysis mechanism of ZrC precursor and fabrication of C/C-ZrC composites by precursor infiltration and pyrolysis. Trans. Nonferrous Metals Soc. China. **24**(6), 1779–1784 (2014)
69. He, R., Ding, G., Zhang, K., Li, Y., Fang, D.: Fabrication of SiC ceramic architectures using stereolithography combined with precursor infiltration and pyrolysis. Ceram. Int. **45**(11), 14006–14014 (2019)
70. Xie, J., Li, K., Sun, G., Li, H.: Effects of precursor concentration on the microstructure and properties of ZrC modified C/C composites prepared by precursor infiltration and pyrolysis. Ceram. Int. **43**(17), 14642–14651 (2017)
71. Li, Y., Yu, H., Shi, Z., Jin, H., Qiao, G., Jin, Z.: Synthesis of β-SiAlON/h-BN nanocomposite by a precursor infiltration and

pyrolysis (PIP) route. Mater. Lett. **139**, 303–306 (2015). https://doi.org/10.1016/j.matlet.2014.10.113
72. Y. Li, D. Liu, Y. Cai, D. Ding, Z. Wu, and G. Xiao, "Improved thermal shock resistance of β-SiAlON/h-BN composite prepared by a precursor infiltration pyrolysis (PIP) route," Ceram. Int., vol. **46**, no. 10, Part B, pp. 16932-16937, 2020/07/01/ 2020, https://doi.org/10.1016/j.ceramint.2020.03.273.
73. E. Grigoryev, V. Goltsev, K. Smirnov, D. Moskovskikh, and A. Sedegov, "β-SiAlON-based ceramic composites by combustion synthesis and spark plasma sintering," 2019.
74. Yeh, C.L., Sheng, K.C.: Effects of α-Si3N4 and AlN addition on formation of α-SiAlON by combustion synthesis. J. Alloys Compd. **509**(2), 529–534 (2011)
75. Zhou, C.R., Yu, Z.B., Krstic, V.D.: Pressureless sintered self-reinforced Y-α-SiAlON ceramics. J. Eur. Ceram. Soc. **27**(1), 437–443 (2007). https://doi.org/10.1016/j.jeurceramsoc.2006.04.185
76. Liu, G., Chen, K., Zhou, H., Ning, X., Pereira, C., Ferreira, J.M.F.: Preparation of Ca α-SiAlON powders with rod-like crystals by combustion synthesis. Ceram. Int. **32**(4), 411–416 (2006). https://doi.org/10.1016/j.ceramint.2005.03.017
77. Smirnov, K.L., Grigoryev, E.G., Nefedova, E.V.: β-SiAlON-Based Ceramic Composites from Combustion-Synthesized Raw Materials by Spark Plasma Sintering. Adv. Mater. Technol. **3**, 26–28 (2018)
78. Ma, B.-Y., Sun, M.-G., Ding, Y.-S., Yan, C., Li, Y.: Fabrication of β-Sialon/ZrN/ZrON composites using fly ash and zircon. Trans. Nonferrous. Metals Soc. China. **23**(9), 2638–2643 (2013). https://doi.org/10.1016/S1003-6326(13)62779-X
79. Yin, L., Jones, M.I.: The formation and properties of Sialon-ZrN composites produced by reaction bonding combined with post gas-pressure sintering. Ceram. Int. **44**(9), 10753–10761 (2018)
80. Huang, J., et al.: Preparation and blast furnace slag corrosion behavior of SiC–Sialon–ZrN free-fired refractories. Ceram. Int. **40**(7, Part A), 9763–9773 (2014). https://doi.org/10.1016/j.ceramint.2014.02.063
81. Sun, Q., et al.: High-performance TiN reinforced Sialon matrix composites: a good combination of excellent toughness and tribological properties at a wide temperature range. Ceram. Int. **44**(14), 17258–17265 (2018)
82. Zhang, L., et al.: Effect of ZrO2 on the physicochemical properties and biological properties of β-SiAlON–ZrO2 composite ceramics. Ceram. Int. **47**(1), 1244–1252 (2021). https://doi.org/10.1016/j.ceramint.2020.08.244
83. Lao, X., Xu, X., Jiang, W., Liang, J., Miao, L., Leng, G.: Effects of various sintering additives on the properties of β-SiAlON–SiC ceramics obtained by liquid phase sintering. Ceram. Int. **47**(9), 13078–13092 (2021). https://doi.org/10.1016/j.ceramint.2021.01.172
84. Acikbas, N.C.: Tribological behavior of αı/βı-SiAlON-TiN composites. J. Eur. Ceram. Soc. **38**(5), 2279–2288 (2018). https://doi.org/10.1016/j.jeurceramsoc.2018.01.013
85. Amin, M., Ehsani, N., Mozafarinia, R.: Effect of seeding and carbon content on the formation and microstructure of Ca-α-SiAlON. Int. J. Refract. Met. Hard Mater. **82**, 208–214 (2019). https://doi.org/10.1016/j.ijrmhm.2019.04.021
86. Syed, H.S., Abubakar, A.A., Hakeem, A.S.: A Material-by-Design Approach to Develop Ceramic-and Metallic-Particle-Reinforced Ca-α-SiAlON Composites for Improved Thermal and Structural Properties. Nanomaterials. **12**(13), 2176 (2022)
87. Wang, Y., Wan, W., Mao, J., Tian, L., Li, R.: Microstructure and Wear Behavior of Plasma-Sprayed TiO2–SiAlON Ceramic Coating. Coatings. **10**(12), (2020). https://doi.org/10.3390/coatings10121268
88. Hotta, M., Goto, T.: Preparation of β SiAlON-cBN Composites by Spark Plasma Sintering. Key Eng. Mater. **403**, 241–242 (2009). https://doi.org/10.4028/www.scientific.net/KEM.403.241
89. Abd El-Mageed, H.R., Abbas, H.S.: Adsorption behavior of mercaptopurine and 6-thioguanine drugs on the B12N12, AlB11N12 and GaB11N12 nanoclusters, a comparative DFT study. J. Biomol. Struct. Dyn. 1–20 (2021). https://doi.org/10.1080/07391102.2021.1930163
90. M. H. Moradi, M. Aliofkhazraei, M. T. Farani, A. Aolgoon, and A. S. Rouhaghdam, "Investigation of Anticorrosion Properties of Epoxy-SiAlON Nanocomposite Powder Coating Fabricated by Electrostatic Spraying Method," 2016.
91. Zheng, G., Zhao, J., Gao, Z., Cao, Q.: Cutting performance and wear mechanisms of Sialon–Si3N4 graded nano-composite ceramic cutting tools. Int. J. Adv. Manuf. Technol. **58**(1), 19–28 (2012). https://doi.org/10.1007/s00170-011-3379-2
92. Tian, Z., Duan, X., Yang, Z., Ye, S., Jia, D., Zhou, Y.: Microstructure and erosion resistance of in-situ SiAlON reinforced BN-SiO2 composite ceramics. J Wuhan Univ Technol-Mater. Sci. Ed. **31**(2), 315–320 (2016). https://doi.org/10.1007/s11595-016-1369-9
93. Hmelov, A.V.: Sintering a Mixture of Powders in the Al2O3–SiO2–β-SiAlON–TiC–Dy2O3 System by the Spark-Plasma Method with High Compaction Loading. Refract. Ind. Ceram. **60**(3), 284–290 (2019). https://doi.org/10.1007/s11148-019-00354-6
94. Biswas, M., Sarkar, S., Bandyopadhyay, S.: Densification, Microstructure, and Tribomechanical Performance of SPS-Processed 27R-SiAlON Polytype-Reinforced AlN: A Comparison Between Continuous and Pulsed Direct Current Mode. Metall. Mater. Trans. A. **50**(5), 2381–2390 (2019). https://doi.org/10.1007/s11661-019-05174-4
95. Syed, H.S., Hakeem, A.S., Qadeer, A., Ehsan, M.A.: "CaO/Yb2O3-doped SiAlONs synthesized with crystalline and amorphous Si3N4 using spark plasma sintering," MRS. Communications. **12**(3), 295–301 (2022). https://doi.org/10.1557/s43579-022-00172-x
96. Smirnov, K.L.: β-SiAlON–BN composites by infiltration-mediated SHS under high pressure of nitrogen gas. Int. J. Self-Propag. High-Temp Synth. **25**(1), 17–22 (2016). https://doi.org/10.3103/S1061386216010131
97. Nefedova, E.V., Grigoryev, E.G., Fokin, D.A., Smirnov, K.L.: Spark plasma sintering of β-SiAlON–BN composites from combustion-synthesized powders. Int. J. Self-Propag. High-Temp Synth. **25**(4), 229–233 (2016). https://doi.org/10.3103/S1061386216040075
98. Shi, X.F., Cai, Z.X., He, C., Wang, J.J., Yue, X.Y., Ru, H.Q.: Effect of Y2O3 on Microstructure and Properties of cBN/SiAlON Composite. Key Eng. Mater. **655**, 22–26 (2015). https://doi.org/10.4028/www.scientific.net/KEM.655.22
99. Wu, X.Z., Wu, Y., Han, J.L., Shen, T.Y.: Microstructures and Mechanical Properties of β-Sialon-cBN Composites. Key Eng. Mater. **697**, 515–520 (2016). https://doi.org/10.4028/www.scientific.net/KEM.697.515
100. Zhu, L., Chen, K., Huang, Z.H., Fang, M.H., Liu, Y.G.: Influence of Aluminum Contents on Phase Behavior and Properties of TiN-Sialon-Corundum Composites by Aluminothermic Reduction Nitridation. Key Eng. Mater. **633**, 57–60 (2015). https://doi.org/10.4028/www.scientific.net/KEM.633.57
101. Qin, Y., Liu, X., Zhang, Q., Zhao, F., Liu, X., Jia, Q.: Oxidation kinetics of bauxite-based β-SiAlON with different particle sizes. Corros. Sci. **166**, 108446 (2020)
102. Wang, G., Shan, Y., Xu, J., Chen, Y., Xu, J., Li, J.: Joining of AlON ceramics by using β-SiAlON/Y-Si-Al-ON glass-ceramic as interlayer. J. Non-Cryst. Solids. **503**, 389–396 (2019)

103. M. Biswas, S. Sarkar, R. Halder, S. Bysakh, K. Muraleedharan, and S. Bandyopadhyay, "Sintering and characterization of a hard-to-hard configured composite: Spark plasma sintered WC reinforced α−SiAlON," J. Phys. Chem. Solids, vol. **145**, p. 109548, 2020/10/01/ 2020, https://doi.org/10.1016/j.jpcs.2020.109548.
104. Sarkar, S., Biswas, M., Halder, R., Bandyopadhyay, S.: Spark plasma sintering processed α−SiAlON bonded tungsten carbide: Densification, microstructure and tribomechanical properties. Mater. Chem. Phys. **248**, 122955 (2020). https://doi.org/10.1016/j.matchemphys.2020.122955
105. Song, S., et al.: The adhesion strength and mechanical properties of SiC films deposited on SiAlON buffer layer by magnetron sputtering. Surf. Coat. Technol. **360**, 116–120 (2019)
106. Yang, Z., Yu, L., Shang, Q., Liu, M., Dai, Z.: Effect of La2O3 addition on densification behavior and properties of Mg-doped sialon. Ceram. Int. **44**(1), 814–820 (2018)
107. Sarkar, S., Halder, R., Biswas, M., Bandyopadhyay, S.: Densification, microstructure and tribomechanical properties of SPS processed β-SiAlON bonded WC composites. Int. J. Refract. Met. Hard Mater. **92**, 105318 (2020)
108. Qin, H., et al.: Role of the vapour phases in the formation mechanism of 15R-SiAlON in FexSiy-Si3N4-Al2O3 composites at 1800° C. Ceram. Int. **44**(18), 23239–23247 (2018)
109. Yin, C., Zhang, J., Li, X., Chen, P., Zhu, B.: Simulation and experimental investigation of preferred β-Sialon growth and its effects on thermo-mechanical properties of Al2O3–C refractories. Ceram. Int. **45**(14), 17298–17304 (2019)
110. Zhang, J., Li, X., Chen, P., Zhu, B.: Formation mechanism of β-Sialon with different morphologies based on DFT calculation and its effect on the performance of refractory composites. Ceram. Int. **46**(2), 1836–1843 (2020). https://doi.org/10.1016/j.ceramint.2019.09.160
111. Yin, C., Li, X., Chen, P., Zhu, Y., Zhu, B.: Morphological regulation and simulation of β-Sialon and its effect on thermo-mechanical properties of Al2O3-C refractories. Ceram. Int. **46**(10), 14597–14604 (2020)
112. Zhang, J., Li, X., Gong, W., Chen, P., Zhu, B.: First-principles simulation of the growth of in situ synthesised β-Sialon and its effects on the thermo-mechanical properties of Al2O3-C refractory composites. J. Eur. Ceram. Soc. **39**(8), 2739–2747 (2019)
113. Zhang, M., et al.: In situ nitriding reaction formation of β-Sialon with fibers using transition metal catalysts. Ceram. Int. **45**(17, Part A), 21923–21930 (2019). https://doi.org/10.1016/j.ceramint.2019.07.204
114. Khan, R.M.A., Ahmed, B.A., Al Malki, M.M., Hakeem, A.S., Laoui, T.: Synthesis of hard and tough calcium stabilized α-sialon/SiC ceramic composites using nano-sized precursors and spark plasma sintering. J. Alloys Compd. **757**, 200–208 (2018)
115. Zheng, G., Zhao, J., Zhou, Y.: Friction and wear behaviors of Sialon–Si3N4 graded nano-composite ceramic materials in sliding wear tests and in cutting processes. Wear. **290-291**, 41–50 (2012). https://doi.org/10.1016/j.wear.2012.05.020
116. Ma, H., Bao, C.: Preparation, oxidation property and mechanism of Si3N4/O′-SiAlON composite ceramics. Ceram. Int. **47**(11), 15383–15391 (2021). https://doi.org/10.1016/j.ceramint.2021.02.103
117. Kushan Akin, S.R., Turan, S., Gencoglu, P., Mandal, H.: Effect of SiC addition on the thermal diffusivity of SiAlON ceramics. Ceram. Int. **43**(16), 13469–13474 (2017). https://doi.org/10.1016/j.ceramint.2017.07.051
118. Kaya, P., et al.: An alternative composite approach to tailor the thermoelectric performance in SiAlON and SiC. J. Eur. Ceram. Soc. **37**(10), 3367–3373 (2017). https://doi.org/10.1016/j.jeurceramsoc.2017.04.004
119. Shao, Y., Li, X., Ji, H., Sun, X., Cao, P.: Effect of α-Al2O3 on in situ synthesis low density O′-sialon multiphase ceramics. J. Alloys Compd. **509**(33), 8345–8349 (2011). https://doi.org/10.1016/j.jallcom.2011.02.143
120. Yurdakul, H., Turan, S.: Identification of Ti incorporation into β-SiAlON crystal structure through transmission electron microscopy techniques. Ceram. Int. **38**(7), 5807–5811 (2012). https://doi.org/10.1016/j.ceramint.2012.04.028
121. Jiang, T., Xue, X.-X., Li, Z.-F., Duan, P.-N.: High temperature oxidation behavior of electroconductive TiN/O′-Sialon ceramics prepared from high titania slag-based mixture. Trans. Nonferrous Metals Soc. China. **21**(12), 2638–2643 (2011). https://doi.org/10.1016/S1003-6326(11)61103-5
122. Ahmed, B.A., et al.: Effect of precursor size on the structure and mechanical properties of calcium-stabilized sialon/cubic boron nitride nanocomposites. J. Alloys Compd. **728**, 836–843 (2017). https://doi.org/10.1016/j.jallcom.2017.09.032
123. Garrett, J.C., Sigalas, I., Herrmann, M., Olivier, E.J., O'Connell, J.H.: cBN reinforced Y-α-SiAlON composites. J. Eur. Ceram. Soc. **33**(11), 2191–2198 (2013). https://doi.org/10.1016/j.jeurceramsoc.2013.03.014
124. An, J., Ge, T., Xu, E., Zhao, F., Liu, X.: Preparation and properties of mullite-SiC-O′-SiAlON composites for application in cement kiln. Ceram. Int. **46**(10, Part A), 15456–15463 (2020). https://doi.org/10.1016/j.ceramint.2020.03.090
125. Huang, C.M., Zhu, D., Yuren, X., Kriven, W.M., Yuh, C.Y.: SiCf/O′-SiAlON composite: properties and oxidation retained properties. Mater. Sci. Eng. A. **220**(1), 176–184 (1996). https://doi.org/10.1016/S0921-5093(96)10477-9
126. Sun, X.L., Sun, K.N., Du, M., Li, A.M.: The Effect of Fe3Al on the Microstructure and Mechanical Properties of β-Sialon Ceramic. Adv. Mater. Res. **487**, 775–780 (2012)
127. Choi, J.-H., Lee, S.-M., Nahm, S., Kim, S.: Effect of Y2O3 content on the microstructural characteristics and the mechanical and thermal properties of Yb-doped SiAlON ceramics. Ceram. Int. **48**(9), 12161–12169 (2022). https://doi.org/10.1016/j.ceramint.2022.01.077
128. Yang, J., Xue, X., Jiang, T., Xie, P., Wang, M.: Preparation of in-situ TiO2/O′-Sialon multiphase ceramics by selective-oxidation. Ceram. Int. **32**(5), 533–538 (2006). https://doi.org/10.1016/j.ceramint.2005.04.007
129. Wu, J., Zhang, Y., Xu, X., Lao, X., Li, K., Xu, X.: A novel in-situ β-Sialon/Si3N4 ceramic used for solar heat absorber. Ceram. Int. **41**(10, Part B), 14440–14446 (2015). https://doi.org/10.1016/j.ceramint.2015.07.080
130. Hmelov, A.V.: Synthesis and Properties of Mullite–Sialon–ZrB2Materials Produced Using a Spark-Plasma Technique. Refract. Ind. Ceram. **59**(6), 633–641 (2019)
131. Yin, L., Zhao, K., Ding, Y., Wang, Y., He, Z., Huang, S.: Effect of hBN addition on the fabrication, mechanical and tribological properties of Sialon materials. Ceram. Int. **48**(6), 7715–7722 (2022)
132. Nefedova, E., Grigoryev, E., Fokin, D., Smirnov, K.: SPARK PLASMA SINTERING OF β-SiAlON–BN COMPOSITES. Machines. Technologies. Materials. **10**(10), 41–43 (2016)
133. Hotta, M., Goto, T.: Densification and Phase Transformation of β-SiAlON–Cubic Boron Nitride Composites Prepared by Spark Plasma Sintering. J. Am. Ceram. Soc. **92**(8), 1684–1690 (2009). https://doi.org/10.1111/j.1551-2916.2009.03098.x
134. Hotta, M., Goto, T.: Effect of time on microstructure and hardness of βSiAlON–cubic boron nitride composites during spark plasma sintering. Ceram. Int. **37**(2), 521–524 (2011). https://doi.org/10.1016/j.ceramint.2010.09.051
135. Hayama, S., Ozawa, M., Suzuki, S.: Thermal shock fracture behavior and fracture energy of β′-Sialon-BN composites. J. Ceram. Soc. Jpn. **104**(1213), 828–831 (1996)

136. Barick, P., Saha, B.P.: Effect of Boron Nitride Addition on Densification, Microstructure, Mechanical, Thermal, and Dielectric Properties of β-SiAlON Ceramic. J. Mater. Eng. Perform. **30**(5), 3603–3611 (2021). https://doi.org/10.1007/s11665-021-05692-6
137. Calloch, P., Brown, I.W.M., MacKenzie, K.J.D., Hanna, J.V., Rees, G.J.: Synthesis and properties of new β-Sialon/TiN composites via a novel AlxTiy intermediate. Ceram. Int. **42**(2, Part A), 2330–2338 (2016). https://doi.org/10.1016/j.ceramint.2015.10.029
138. AÇIkbaŞ, N.Ç., AÇIkbaŞ, G.: Dependence of SiAlON-TiN Composite Properties on TiN Reinforcement Particle Sizes. Anadolu Univ. J. Sci. Technol. A-Appl. Sci. Eng. **19**(2), 356–367 (2018)
139. Nekouee, K.A., Khosroshahi, R.A.: Preparation and characterization of β-SiAlON/TiN nanocomposites sintered by spark plasma sintering and pressureless sintering. Mater. Des. **112**, 419–428 (2016). https://doi.org/10.1016/j.matdes.2016.09.090
140. Kandemir, A., Sevik, C., Yurdakul, H., Turan, S.: First-principles investigation of titanium doping into β-SiAlON crystal in TiN–SiAlON composites for EDM applications. Mater. Chem. Phys. **162**, 781–786 (2015). https://doi.org/10.1016/j.matchemphys.2015.07.003
141. Yurdakul, H., Turan, S., Ayas, E., Tunckan, O., Kara, A.: Analytical transmission electron microscopy observations on the stability of TiCN in electrically conductive α-β SiAlON/TiCN composites. J. Eur. Ceram. Soc. **34**(12), 2905–2911 (2014). https://doi.org/10.1016/j.jeurceramsoc.2014.03.024
142. Acikbas, N.C., Tegmen, S., Ozcan, S., Acikbas, G.: Thermal shock behaviour of α:β-SiAlON–TiN composites. Ceram. Int. **40**(2), 3611–3618 (2014). https://doi.org/10.1016/j.ceramint.2013.09.064
143. Deng, X., Li, X., Zhu, B., Chen, P.: In-situ synthesis mechanism of plate-shaped β-Sialon and its effect on Al2O3–C refractory properties. Ceram. Int. **41**(10), 14376–14382 (2015)
144. Rambo, C.R., Sieber, H.: Manufacturing of cellular β-SiAlON/β-SiC composite ceramics from cardboard. J. Mater. Sci. **41**(11), 3315–3322 (2006). https://doi.org/10.1007/s10853-005-5428-4
145. Wei, X., et al.: Phenomenon of Whiskers Formation in Al2O3−C Refractories. Adv. Eng. Mater. **24**(2), 2100718 (2022)
146. Si, Y., et al.: Thermodynamic calculation and microstructure characterization of spinel formation in MgO–Al2O3–C refractories. Ceram. Int. **48**(11), 15525–15532 (2022)
147. Zhu, B., Zhu, Y., Li, X., Zhao, F.: Effect of ceramic bonding phases on the thermo-mechanical properties of Al2O3–C refractories. Ceram. Int. **39**(6), 6069–6076 (2013)
148. Lan, Y.L., et al.: Mechanical properties and thermal conductivity of dense β-SiAlON ceramics fabricated by two-stage spark plasma sintering with Al2O3-AlN-Y2O3 additives. J. Eur. Ceram. Soc. **40**(1), 12–18 (2020). https://doi.org/10.1016/j.jeurceramsoc.2019.09.013
149. Kovziridze, Z., et al.: Preparation of Composites by Nitro Aluminothermic Processes, over β–SiAlON Matrix in the SiAlON-SiC-Al2O3 System. J. Electron. Cool. Thermal. Ctrl. **6**(2), 62–77 (2016)
150. Yang, Z., et al.: Optical and mechanical properties of Mg-doped sialon composite with La2O3 as additive. J. Eur. Ceram. Soc. **32**(4), 931–935 (2012). https://doi.org/10.1016/j.jeurceramsoc.2011.10.020
151. Takatori, K.: Thermal shock resistance of alumina-sialon composites. J. Mater. Sci. **29**(8), 2115–2118 (1994)
152. Adeniyi, A.S., et al.: The property characterization of α-sialon/Ni composites synthesized by spark plasma sintering. Nanomaterials. **9**(12), 1682 (2019)
153. Garrett, J.C., Sigalas, I., Herrmann, M.: TEM investigation of the interface formation in cubic boron nitride containing α-SiAlON composites. Ceram. Int. **40**(10, Part B), 16169–16175 (2014). https://doi.org/10.1016/j.ceramint.2014.07.048
154. Garrett, J.C., Sigalas, I., Wolfrum, A.K., Herrmann, M.: Effect of cubic boron nitride grain size in the reinforcing of α-Sialon ceramics sintered via SPS. J. Eur. Ceram. Soc. **35**(2), 451–462 (2015). https://doi.org/10.1016/j.jeurceramsoc.2014.09.036
155. Liu, H., et al.: Significantly enhanced thermal shock resistance of α-Si3N4/O′-Sialon composite coating toughened by two-dimensional h-BN nanosheets on porous Si3N4 ceramics. Ceram. Int. **48**(20), 30510–30516 (2022)
156. Kitabatake, T., Uchikoshi, T., Munakata, F., Sakka, Y., Hirosaki, N.: The optical and mechanical properties of Eu-doped Ca-α-SiAlON phosphor-SiO2 composite films. Trans. Mater. Res. Soc. Japan. **35**(3), 713–716 (2010)
157. Ulucan, U., Ertekin, K., Oğuzlar, S.: Enhancement of optical properties of Lu3Al5O12: Ce3+ and Ca-α-SiAlON: Eu2+ by quinine sulphate. J. Mater. Sci. Mater. Electron. **32**(24), 28176–28191 (2021)
158. Ye, F., Liu, C., Liu, L., Zhou, Y.: Optical properties of in situ toughened ScLu–α-SiAlON. Scr. Mater. **61**(10), 982–984 (2009)
159. Dayan, X.U., Kaikai, Z., Wanyu, Z., Yajuan, F.A.N., Guangqiang, W.: Effect of Micropowder Introduction on Synthesis of SiAlON-bonded SiC Products. China's Refractories. **28**(3), 15 (2019)
160. Ma, H., Bao, C.: Study of mechanical property, oxidation property and mechanism of Si3N4/O′-SiAlON composites fabricated by adding different sizes of SiO2. Corros. Sci. **201**, 110266 (2022). https://doi.org/10.1016/j.corsci.2022.110266
161. Zheng, G., Zhao, J.: Chapter 2 - Performance of Sialon/Si3N4 graded ceramic tools at high speed machining. In: Gupta, K., Davim, J.P. (eds.) High Speed Machining, pp. 27–62. Academic Press (2020)
162. Bitterlich, B., Bitsch, S., Friederich, K.: SiAlON based ceramic cutting tools. J. Eur. Ceram. Soc. **28**(5), 989–994 (2008)
163. Grigoriev, S.N., et al.: Development of DLC-Coated Solid SiAlON/TiN Ceramic End Mills for Nickel Alloy Machining: Problems and Prospects. Coatings. **11**(5), (2021). https://doi.org/10.3390/coatings11050532
164. Robakowska, M., Gierz, Ł., Gojzewski, H.: Sialon and Alumina Modified UV-Curable Coatings with Improved Mechanical Properties and Hydrophobicity. Coatings. **11**(11), (2021). https://doi.org/10.3390/coatings11111424
165. Sabagh, S., Bahramian, A.R., Kokabi, M.: SiAlON nanoparticles effect on the behaviour of epoxy coating. Iran. Polym. J. **21**(4), 229–237 (2012). https://doi.org/10.1007/s13726-012-0020-7
166. Moradi, M.H., Aliofkhazraei, M., Toorani, M., Golgoon, A., Rouhaghdam, A.S.: SiAlON–epoxy nanocomposite coatings: Corrosion and wear behavior. J. Appl. Polym. Sci. **133**(35), (2016). https://doi.org/10.1002/app.43855
167. Yoshimura, K., et al.: Optical properties of solid-state laser lighting devices using SiAlON phosphor–glass composite films as wavelength converters. Jpn. J. Appl. Phys. **55**(4), 042102 (2016)
168. Kitabatake, T., Uchikoshi, T., Munakata, F., Sakka, Y., Hirosaki, N.: Optical and adhesive properties of composite silica-impregnated Ca-α-SiAlON: Eu2+ phosphor films prepared on silica glass substrates. J. Eur. Ceram. Soc. **32**(7), 1365–1369 (2012)
169. Sabagh, S., Bahramian, A.R., Kokabi, M.: SiAlON nanoparticles effect on the corrosion and chemical resistance of epoxy coating. Iran. Polym. J. **21**(12), 837–844 (2012). https://doi.org/10.1007/s13726-012-0095-1
170. Zhang, D.-S., Abadikhah, H., Wang, J.-W., Hao, L.-Y., Xu, X., Agathopoulos, S.: β-SiAlON ceramic membranes modified

with SiO2 nanoparticles with high rejection rate in oil-water emulsion separation. Ceram. Int. **45**(4), 4237–4242 (2019)
171. Zhao, Y.S., Yang, Y., Li, J.T., Borovinskaya, I.P., Smirnov, K.L.: "Combustion synthesis and tribological properties of SiALON-based ceramic composites," International Journal of Self-Propagating High-Temperature. Synthesis. **19**(3), 172–177 (2010). https://doi.org/10.3103/S1061386210030027
172. Xu, X., Wang, D., Rao, Z., Wu, J., Zhou, Y.: In-situ Synthesis and Oxidation Resistance of Sialon/SiC Composite Ceramics Applied as Solar Absorber. J Wuhan Univ Technol.-Mater. Sci. Ed. **36**(1), 6–12 (2021). https://doi.org/10.1007/s11595-021-2371-4
173. Xu, X., Wang, D., Rao, Z., Wu, J., Liu, X., Zhang, C.: Preparation and thermal shock resistance of sialon/SiC composite ceramics used for solar absorber. J. Aust. Ceram. Soc. **57**(2), 359–367 (2021). https://doi.org/10.1007/s41779-020-00537-2
174. Akimune, Y., Hirosaki, N., Ogasawara, T.: Mechanical properties of SiC-particle/sialon composites. J. Mater. Sci. Lett. **10**(4), 223–226 (1991). https://doi.org/10.1007/BF00723811
175. Goto, Y., Fukasawa, T., Kato, M.: Strength of β-sialon/Si3N4 layered composites. J. Mater. Sci. **33**(2), 423–427 (1998). https://doi.org/10.1023/A:1004332132338

Publisher's note Springer Nature remains neutral with regard to jurisdictional claims in published maps and institutional affiliations.